Locating multiple types of charging facilities for battery electric vehicles

Liu, Haoxiang; Wang, David Zhi Wei

2017

Liu, H., & Wang, D. Z. W. (2017). Locating multiple types of charging facilities for battery electric vehicles. Transportation Research Part B: Methodological, in press.

https://hdl.handle.net/10356/83236

https://doi.org/10.1016/j.trb.2017.01.005

Locating multiple types of charging facilities for battery electric vehicles

Haoxiang Liu[a,b], David Z.W. Wang[b,*]

[a] School of Automotive and Transportation Engineering, Hefei University of Technology, Hefei, 230009, China

[b] School of Civil and Environmental Engineering, Nanyang Technological University, 50 Nanyang Avenue, 639798, Singapore

ABSTRACT

To reduce greenhouse gas emissions in transportation sector, battery electric vehicle (BEV) is a better choice towards the ultimate goal of zero-emission. However, the shortened range, extended recharging time and insufficient charging facilities hinder the wide adoption of BEV. Recently, a wireless power transfer technology, which can provide dynamic recharging when vehicles are moving on roadway, has the potential to solve these problems. The dynamic recharging facilities, if widely applied on road network, can allow travelers to drive in unlimited range without stopping to recharge. This paper aims to study the complex charging facilities location problem, assuming the wireless charging is technologically mature and a new type of wireless recharging BEV is available to be selected by consumers in the future other than the traditional BEV requiring fixed and static charging stations. The objective is to assist the government planners on optimally locating multiple types of BEV recharging facilities to satisfy the need of different BEV types within a given budget to minimize the public social cost. Road users' ownership choice among multiple types BEV and BEV drivers' routing choice behavior are both explicitly considered. A tri-level programming is then developed to model the presented problem. The formulated model is first treated as a black-box optimization, and then solved by an efficient surface response approximation model based solution algorithm.

Keywords

Wireless charging, Battery electric vehicle, Charging station location, Vehicle choice, Multi-class user equilibrium, tri-level programming.

1. Introduction

The global climate change due to air pollution stimulates the revolution of the transportation sector. A transition from fossil fuel to cleaner and more energy efficient alternative fuel vehicles is a vital step in reducing the road transportation greenhouse gas emission. Among all the available technologies, electricity has received much attention to substitute the fossil

* Corresponding author. Tel.: +65 67905281; fax: +65 67905281.
E-mail addresses: wangzhiwei@ntu.edu.sg (David Z.W. Wang).

fuel due to its high energy efficiency, as well as the existing widespread electricity grid. The adoption of electric vehicle (EV) grows very fast ever since the introduction of models by global manufacturers, including all-electric or Battery Electric Vehicle (BEV), Plug-in Hybrid Electric Vehicle (PHEV) and other low-emitting electric vehicles. Although the latter two types of EVs have lower emissions as compared to the conventional internal combustion engine vehicle (ICEV), the BEV is a better choice towards the goal of zero-emission to protect the environment. However, the BEV is currently facing several barriers, which include the high purchasing price, extended recharging time and reduced driving range compared to ICEV or even PHEV, as well as lacking of charging facilities.

The most common charging method for BEV is static conductive charging via a cable and a vehicle connector when a BEV is parking. Those chargers can be divided into different classifications according to the power rate used and nationally available power level (Haghbin et al., 2010). Yilmaz and Krein (2013) defined three levels with power rate ranging from 1.4kW to 100kW and the recharging time ranging from more than ten hours to less than half an hour. Apparently, even the expensive level 3 charger, also referred to as fast charging, can hardly compete with the conventional ICEV that could usually be refilled in several minutes. Another type of charging method is battery swapping, which can replace the depleted battery with a fully charged one in less than five minutes. Battery swapping requires huge space for heavy swapping machines, swapping chargers and a few extra EV batteries (Adler and Mirchandani, 2014). More importantly, it requires battery of EV to be easily swapped, which means it should be removable and standardized. However, since the core technologies of BEV lie in its battery packs, it seems very unrealistic for EV companies to do so. In addition to the extended recharging time, the limited range also restricts the public from purchasing BEV. Reports show that the expectations of consumers on alternative fuel vehicle range is at least 300 miles (Deloitte, 2011), while the current BEV battery capacities can generally provide about 100 miles, which cannot satisfy the needs of general consumers (Fuller, 2016).

The existing limitations lead to the studies of other possible charging technologies for BEV, wherein one option is inductive charging or wireless charging. BEVs adopting this technology do not need a cable for recharging and thus are viable for not only static charging (i.e., charging when parking) but also dynamic charging (i.e., charging when moving). Dynamic wireless charging extends driving range and reduces BEVs’ charging time. If the dynamic charging system is widely applied on network, the potential of unlimited driving range may be achieved; other than this, the risk of electric shock will be completely removed (Chawla and Tosunoglu, 2012). Besides, the battery packs capacity may be reduced because the EV can directly get energy from roadway (Wu et al., 2011), and also the speed of EV can be increased due to reduced weight of heavy battery packs. What’s more, dynamic wireless recharging do not require extra urban space, which is extremely desirable for cities with limited land resources, such as Singapore and Hong Kong (Riemann et al., 2015). Because of the advantages of wireless charging, it has attracted much attention from researchers recently but mainly on technical aspects (Budhia et al., 2013; Chen et al., 2015a; Chen et al., 2015b; Onar et al., 2013; Pelletier et al., 2014; Wu et al., 2011; Yilmaz and Krein, 2013).

Only a few existing research works deal with the operational problems related to the practical implementation of wireless charging facilities. Based on the introduction of a wireless charging electric transportation system that was developed at Korea Advanced Institute of Technology (KAIST), a series of researches (Jang et al., 2015; Jang et al., 2012; Jang et al., 2016; Ko and Jang, 2013; Ko et al., 2012; Ko et al., 2015) described the system design and system architecture issues, developed mathematical models to optimize key design parameters in the system, including allocating the power transmitters and evaluating the battery size; and also discussed on the recent advances, commercialization process and further development of wireless charging EV under the background of ITS. What's more, the benefit in the perspective of energy logistics was analyzed qualitatively and economic design optimization models were also developed separately for wireless charging electric transit bus system in closed and open systems. Assuming that high-power, high-efficiency wireless power transfer technologies are mature in the near future, He et al. (2013b) presented mathematical models to determine the optimal prices of electricity and roads to pursue the maximum social welfare. Riemann et al. (2015) investigated optimal locations of a given number of wireless power transfer facilities, aiming to capture the maximum traffic flow on network while considering the road users' routing behavior. Chen et al. (2016) formulated a deployment model with consideration of user equilibrium condition to optimize the locations of wireless charging lanes for a given budget. Fuller (2016) presented a flow-based set covering problem to determine how much dynamic charging facilities are needed in California.

As was in He et al. (2013b), we envision that the wireless recharging technology would be mature in the near future and a new type of wireless recharging BEV is available to be selected by customers. In this situation, when the government authorities plan for locations of the charging facilities for BEV, they should consider deploying different types of charging facilities to meet the need of different BEV types, with considerations of the behaviors of road users. In fact, there are two types of choice behaviors to be taken into consideration: first, as there are multiple types of BEVs in the market, the road users will first decide which type of BEV to purchase; second, road users usually tend to select routes incurring minimum cost for their trips (i.e., travelers' routing behavior). To our best knowledge, no previous research papers in the literature have addressed this charging station location problem considering vehicle ownership of multiple types of BEVs and heterogeneous types of charging facilities. This study aims to fill in this research gap by proposing a tri-level programming approach to explicitly model and solve the location plan of multi-type charging facilities for different BEVs.

Conventional methods in the literature modeled the charging facilities location problems as maximal covering location problem (MCLP) (Church and ReVelle, 1974; Daskin, 2008; Farahani et al., 2012; Hale and Moberg, 2003), flow-capturing location model (FCLM) (Hodgson, 1990), flow-refueling location model (FRLM) (Kuby and Lim, 2005, 2007; Lim and Kuby, 2010), capacitated flow-refueling location model (Upchurch et al., 2009), deviation-flow refueling model (Huang et al., 2015; Kim and Kuby, 2012, 2013), the arc cover path-cover FRLM (Capar et al., 2013), flow-based set covering model (Wang and Lin, 2009) and so on. These location problems do not include the travelers' routing choice behavior. Indeed, only several papers in the literature include transportation network equilibrium in the location problems. He et al. (2013a) allocated a given number of public charging stations for PHEV with consideration of interaction between transportation and power system. He et al. (2015) explored optimally locating public charging stations for BEV considering a tour-based network equilibrium. Lee et al. (2014) developed a model for locating rapid charging stations while considering batters' state of charge and traveling behavior. Besides, a few studies only explored the network equilibrium problem related to EV (He et al., 2014; Jiang and Xie, 2013; Jiang et al., 2014; Jiang et al., 2012). More recently, Nie et al. (2016) presented a mathematical framework for optimizing publicly funded incentive polices on the adoption of plug-in EV.

Specifically, this paper attempts to study the location problem of multiple types of BEV charging facilities, including different levels of plug-in charging stations, static and dynamic wireless charging facilities, with explicit consideration of consumers' choice of multiple types of BEV and multiple classes of BEV users' routing choice behavior. The study aims to assist government planners in determining locations of multiple types of BEV charging stations within a given budget to minimize the public social cost, i.e., maximize the social welfare. A tri-level programming is then developed to model the presented problem. The consumers' choice between different BEV types are described in a logit model, with a utility function related to the government's decision plan on charging facilities location, the income weighted price of different BEV types and the total cost of road users' selected path to accomplish their trip tours. Assuming that travelers select the path with minimum travel cost, as in Wardrop's first principle (Wardrop, 1952), a multi-class user equilibrium (UE) is developed to describe the travelers' routing choice. The pure travel time, recharging time and consumers' income weighted recharging fee are all included in the traveler's total travel cost. Besides, considering that in practice travelers usually utilize dwelling time at destination nodes to recharge BEV (He et al., 2015), we adopt a tour-based approach, which defines a tour as a series of several sequential visited destinations, in the user equilibrium to predict road users' possible recharging.

The developed tri-level model is inherently very difficult to solve. In this paper, we present a novel solution algorithm to solve the developed tri-level programming problem. The model is treated as a black-box optimization problem with a very expensive objective function. The term 'black-box optimization' here refers to a class of optimization problems, where derivative information is unavailable due to lack of explicit functions or high computational cost for derivatives calculation. Then a response surface model based approach, specifically, stochastic radial basis function based algorithm is presented to solve the black-box model, as was introduced in the research of Regis (2011) and Regis and Shoemaker (2007). The response surface models, also called surrogate models, are promising approaches to solve black-box optimization problems. The basic idea of the method is to develop the response surface approximation model for the expensive black-box function, thus the information from the response surface model can be utilized to guide the search for the optimum of the original problem. This type of solution algorithm belongs to the category of derivative-free optimization and have been applied in many research areas ranging from finite-element or partial-differential equation systems, to groundwater supply, to supply chain optimization and so on (Boukouvala et al., 2015; Fowler et al., 2008; Wan et al., 2005). Chen et al. (2014) applied surrogate-based approaches to solve highway toll charges problem in transportation network. The presented response surface model based algorithm is very efficient in solving the developed model, because it only needs to evaluate the expensive black-box function once in each iteration while the majority of computational time is consumed in black-box function evaluation. The expensive black-box function evaluation procedure embedded in each iteration of the algorithm, is solved by a fixed-point method for the EV choice model and an MSA based method for the lower-level user equilibrium problem. Two sub-problems are developed for wireless charging EV and plug-in charging EV, respectively, to generate the shortest path plans with minimum travel cost in the process of solving the network equilibrium. We contend that the proposed response surface model based solution algorithm can be easily extended to solve other complex transportation problems with equilibrium constraints, which are usually formulated as multi-level mathematical programming.

The following sections are organized as follows. In Section 2, the tri-level model is developed for the proposed multiple types EV charging station location problem. Section 3 presents the stochastic radial basis function surrogate model based solution algorithm to solve the developed model. The expensive black-box evaluation is also stated in this section. Numerical examples and results are described in Section 4. Finally, Section 5 concludes the paper.

2. Model formulation

The following notations are utilized in the model formulation section.

Decision variables:

x_a	Traffic flow on link a.
t_a	Travel time on link a.
$t_{m,v}^{p,q}$	Travel time of path p of tour q for class m users choosing EV type v.
$s_{m,v}^{p,q}$	Recharging delay on path p of tour q for class m users choosing EV type v.
$c_{m,v}^{p,q}$	Recharging fee of path p of tour q for class m users choosing EV type v.
$y_{\psi,i}^{plu}$	Whether a plug-in charging station of type ψ should be built at node i. $y_{\psi,i}^{plu}=1$ if a station should be built; otherwise $y_{\psi,i}^{plu}=0$. The same binary relationship is applied to y_i^{wlss} and y_a^{wlsd}.
y_i^{wlss}	Whether a wireless static charging station for wireless EV should be built at node i.
y_a^{wlsd}	Whether a dynamic charging lane for wireless EV should be built on link a.
$u_{m,v}^{q}$	Utility of tour q users choosing EV type v.
$\lambda_{m,v}^{q}$	Probability of tour q users choosing EV type v.

$f_{m,v}^{p,q}$ Path flow on path p of tour q for class m users choosing EV type v.

Sets, index, coefficients and parameters:

w_m^o Average wage rate in unit of dollar per hour of class m users.

w_m^y Average income per year of class m, which is equal to $w_m^y = w_m^o \times 40 \times 52$.

β_g The coefficient for vehicle price in the logit model, should be non-positive.

$\beta_{t,m}$ The coefficient for total traveling cost of each class of users, including travel time, recharging delay and recharging fee, should be non-positive.

β_q The constant that incorporates other tour related cost and is regardless of vehicle choice

G_v Purchasing cost of EV type v, including vehicle price g_v^{car} and charging equipment cost g_v^{equ}.

l_v Average life time of EV type v.

γ_m^q $\gamma_m^q = d_m^q / d^q \ \forall m, q$ is a given ratio of class m users to the tour q demand.

π The tour plan with minimum total travel cost.

ψ Set of feasible types of plug-in charging stations; $\psi \in \Psi = \{1, 2, 3\}$, where 1, 2 and 3 refer to the level 1, 2, and 3 charging stations, respectively.

N Set of nodes on the network.

N_1 Set of candidate nodes where plug-in charging stations can be built.

N_2 Set of candidate nodes where stationary wireless charging stations can be built.

A Set of links on the network.

A_1 Set of candidate links for building dynamic wireless charging lanes.

Φ Government budget limit for building EV charging facilities.

$b_{\psi,i}^{plu}$ Cost of building a plug-in charging station of type ψ at node i.

b_a^{wlsd} Cost of building dynamic wireless charging facilities on link a.

b_i^{wlss} Cost of building a stationary wireless charging station at node i.

τ The weighted factor of EV trip failure cost.

d^q Total travel demand of tour q.

$d_{m,v}^q$ Travel demand of class m travellers using vehicle v traveling along tour q

t_a^0 Free-flow travel time of link a.

$\delta_{m,v,a}^{OD,p,q}$ An indicator equals to 1 if link a is on a path p connecting an OD along a tour q for class m travellers using EV type v, and 0 otherwise.

$P_{m,v}^q$ Set of available paths for class m users of tour q.

In this problem, the government authorities make decisions on where and which type of EV recharging facility to be located aiming to minimize the social cost. The resulting location plan has a significant impact on consumers' choices of EV type and thus their routing choices. For the road users, it is assumed that all the travelers tend to purchase one type of EV first. They will seek to pay least to finish their own usual tour schedules. To this end, the travelers will consider both the government's investment on EV recharging facilities and their own tour when choosing a type of EV with different charging methods. Finally, as road users, they will select the route with minimum travel cost, including travel time, recharging fee and delay time. The relationship between these three decisions is illustrated in Figure 1. The government plays as a leader in the upper-level and make decision on EV recharging facility location plan. The road users then act in the middle-level and decide which type of EV to purchase. In the lower-level, a user equilibrium model is then applied to describe the road users' choice of route and recharging plan with minimum individual travel cost. Apparently, the upper-level location plan impacts the decision of traveler's choice of EV type and tour route. In turn, the road users' choice of tour routes in the lower-level will affect the government's decision on locating EV charging stations and the users' own EV type choice. To explicitly describe the relationship, a tri-level mathematical programming approach is then applied as below to model the problem, whose resultant solution would assist the government to make better decision.

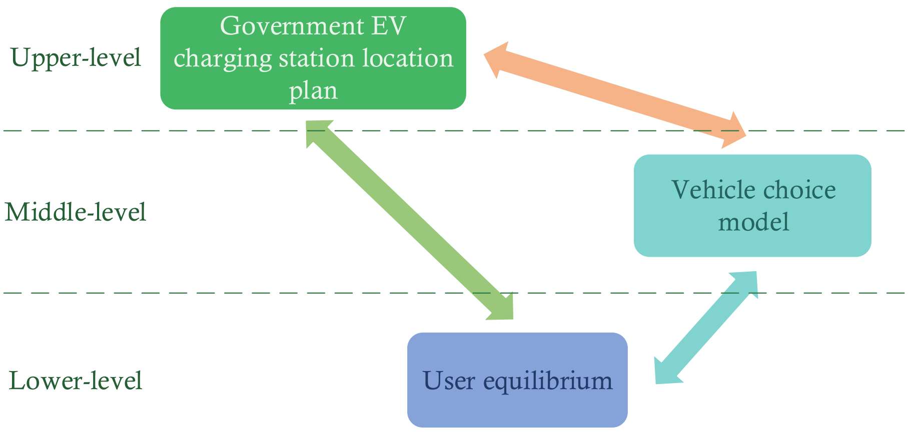

Figure 1 The relationship between the three levels.

2.1 Upper-level programming for EV location decision

The government locates the multiple types of EV charging facilities to pursue the maximum the social welfare, i.e., minimum the social cost. Hence, the objective function of the whole model is represented by (1), which is a weighted function of total travel cost and penalty fee of failed trips. The first term is the total travel cost of all finished trips, including driving time, income weighted recharging fee and extra delay time due to recharging behavior in the tour of all user classes choosing different types of EVs, where x_a and t_a represent the traffic flow and travel time on link a respectively; A is the set of links on the network; $VMQ(\mathbf{y})$ is the set of finished trips for each combination of EV type v, user class m of tour q given a location plan $\mathbf{y}=(y_{\psi,i}^{plu}, y_i^{wlss}, y_a^{wlsd})$. $y_{\psi,i}^{plu}, y_i^{wlss}$ and y_a^{wlsd} are all binary variables which indicate whether or not a type of charging station is built at a specific location; $y_{\psi,i}^{plu}$ represents whether a plug-in charging station of type ψ should be built at node i; ψ is the set of feasible types of plug-in charging stations, $\psi \in \Psi = \{1,2,3\}$, where 1, 2 and 3 refer to the level 1, 2, and 3 charging stations, respectively; y_i^{wlss} defines whether a wireless static charging station for wireless EV should be built at node i; y_a^{wlsd} stands for indicator whether a dynamic charging lane for wireless EV should be built on link a. P_m^q refers to the set of available paths for class m users of tour q. Here, classes of users are categorised by initial state of charge of EV battery, buffer range, and average income; while the type of EV is classified by charging method, that is, plug-in or wireless recharging. $f_{m,v}^{p,q}$ is the path flow of path p of tour q for class m users choosing EV type v; $t_{m,v}^{p,q}$ is the travel time of path p; $s_{m,v}^{p,q}$ and $c_{m,v}^{p,q}$ stand for recharging delay and recharging fee on path p of tour q for class m users choosing EV type v, respectively. The original dwelling time at destination nodes is not counted in the delay time here. This is more reasonable in practice, for example, people will recharge their EV when they are working or shopping. The second term represents the penalty fee for all failed trips. Here, it is assumed that the government stands for the public interests and it is desirable that all trip demands are satisfied. τ is the weighted factor of penalty fee for all failed trips, up to the government for the purpose of adjusting the balance between the two terms. $d_{m,v}^q$ is the travel demand of class m travellers using vehicle v traveling along tour q; $\rho_{m,v}^q$ is the penalty fee for class m users of tour q choosing vehicle type v if they fail to complete their tour.

Constraint (2) is the budget limit of the government, where Φ represents the total budget for construction cost of all types of EV charging facilities to be built at candidate locations; $b_{\psi,i}^{plu}$ is the cost of building a plug-in charging station of type ψ at node i; b_a^{wlsd} represents the cost of building dynamic wireless charging facilities on link a; b_i^{wlss} is the cost of building a stationary wireless charging station at node i; N_1 defines the set of candidate nodes where plug-in charging stations can be built; N_2 is the set of candidate nodes where stationary wireless charging stations can be built; A_1 is the set of candidate links for building dynamic wireless charging lanes. It is assumed that two types of EVs are considered in this paper, the plugin charging EV and the wireless charging EV. The plugin charging EV can be recharged via level 1, 2, or 3 charges at charging station, while the wireless charging EV can be recharged via either static inductive charger at charging stations or dynamic recharging when driving on special charging links. Constraint (3) indicates the binary constraint for the decision variables. All the information needed in (1), including link flow, link travel time, travel cost for each class of users, demand assignment for different EV types, as well as whether or not a trip is failed, is derived from the middle-level and lower-level programing.

$$\min \quad (1-\tau)\left(\sum_{a\in A} x_a t_a + \sum_{v,m,q\in VMQ(\mathbf{y})} \sum_{p\in P_{m,v}^{q}(\mathbf{y})} f_{m,v}^{p,q}\left(s_{m,v}^{p,q} + c_{m,v}^{p,q} / w_m^o\right)\right) + \tau \sum_{v,m,q\notin VMQ(\mathbf{y})} d_{m,v}^{q} \rho_{m,v}^{q} \tag{1}$$

Subject to:

$$\sum_{\psi\in\Psi} \sum_{i\in N_1} b_{\psi,i}^{plu} y_{\psi,i}^{plu} + \sum_{i\in N_2} b_i^{wlss} y_i^{wlss} + \sum_{a\in A_1} b_a^{wlsd} y_a^{wlsd} \le \Phi \tag{2}$$

$$y_{\psi,i}^{plu}, y_i^{wlss}, y_a^{wlsd} \in \{0,1\} \quad \forall \psi, i, a \tag{3}$$

2.2 Middle-level programming for consumers' EV choice

In the middle-level programming, road users' choice of different EV types is considered, that is whether to buy a plug-in charging EV or a wireless charging EV. Constraint (4) calculates the probability of tour q road users m choosing vehicle type v following the logit function, where $\lambda_{m,v}^{q}$ is the probability of class m users of tour q choosing EV type v and $u_{m,v}^{q}$ is the utility of class m users choosing EV type v in tour q. The definition of utility $u_{m,v}^{q}$ is stated in constraint (5), which consists of average income weighted purchasing price of a type of EV and the total travel cost of each class users by using this type of EV to finish tour q. In this constraint, β_g in the first term represents the coefficient for EV purchasing price, while $\beta_{t,m}$ in the second term stands for the coefficient for total travel cost of user class m, and β_q in the last term can incorporate other tour related cost regardless of vehicle choice. Note that all the coefficients should be non-positive. G_v is the purchasing cost of EV type v, including vehicle price g_v^{car} and its charging equipment cost g_v^{equ}, that is, $G_v = g_v^{car} + g_v^{equ}$. Here, it is assumed that, if wireless charging EV is selected, charging equipment, which is required either in stationary charging station or on dynamic charging lane, both need to be purchased by the EV users. l_v stands for the average life time of EV type v. w_m^y represents the average income per year for class m users and w_m^o is the average wage rate in unit of dollar per hour for class m users; the relationship $w_m^y = w_m^o \times 40 \times 52$ exists between the two parameters. The term $\dfrac{G_v}{l_v w_m^y}$ stands for the average income weighted yearly purchasing price of EV type v over its life expectance l_v for class m users. π in constraint (5) is the tour plan with minimum total travel cost of class m user of tour q driving EV type v. This plan is obtained from the lower-level programing of user network equilibrium. Finally, the demand $d_{m,v}^{q}$ of each class m using vehicle type v of tour q can be calculated through the following equation (6), where d^q is the total travel demand of tour q and γ_m^q is the percentage of class m users of tour q, which can be obtained via statistical data in practice.

$$\lambda_{m,v}^q = \frac{\exp(u_{m,v}^q)}{\sum_{v \in V} \exp(u_{m,v}^q)} \quad \forall m, v, q \tag{4}$$

$$u_{m,v}^q = \frac{\beta_g G_v}{l_v w_m^y} + \beta_{t,m}\left(t_{m,v}^{\pi,q} + s_{m,v}^{\pi,q} + \frac{c_{m,v}^{\pi,q}}{w_m^o}\right) + \beta_q \quad \forall m, v, q \tag{5}$$

$$d_{m,v}^q = d^q \gamma_m^q \lambda_{m,v}^q \quad \forall q, m, v \tag{6}$$

2.3 Lower-level programing for network equilibrium with multiple classes of users

In the lower-level programming, a user equilibrium model is developed for multiple classes of users' routing choice behavior with different types of EVs. Not only travel time and EV drivers' range anxiety, but EVs' recharging fee and delay time are also considered in this routing choice model. For each type of EV, a trip can be finished if there is at least one viable path existing that either the EV has enough electricity stored in its battery or it can be recharged with sufficient electricity to complete the path. It is reasonable to assume that the road users can hardly predict the relationship between energy consumption and traffic flow on link, that is, they assume the amount of electricity consumed on a link is fixed to make their decisions rather than calculate the accurate energy consumption via complicated calculation process. (The readers who are interested in the network equilibrium considering flow-dependent energy consumption can refer to He et al. (2014).) Under this assumption, the amount of electricity needed to complete a given path is a known constant, which can be calculated in priori. It is also reasonable to assume that the recharging fee and recharging time are both linear functions and strictly increasing with respect to the electricity recharged, depending on which type of charging facility utilized.

Another interesting aspect that is also considered in the lower-level user equilibrium is the adoption of sequential trips rather than single trips. Conventional user equilibrium deals with trips between different OD pairs separately, assuming there is no relationship between the trips. However, this is not true because trips between different OD pairs may be finished by the same traveler. Thus the user's behavior at the first destination node and also the second origination node is not correctly considered if traditional user equilibrium is adopted. In practice, traveler may sequentially visit different destinations and utilize their dwelling time at these nodes to recharge their EV batteries. For example, people will charge EV at their work place or when they are shopping. In this situation, the recharging time that is less than the users' original dwelling time should not be counted in the recharging delay. Considering this aspect in the UE model will helps the government to better locate the EV charging stations so as to satisfy the need of the public.

Suppose road users always choose the path with minimum travel cost to finish their trips, where the travel cost consists of pure travel time, recharging delay and recharging fee. Hence, following the rule of Wardrop's first principle (Wardrop, 1952), we can define the multi-class users' network equilibrium as below. At equilibrium, for the same class of travelers using the same type of EV, the tour travel costs of all utilized paths are equal to the minimum travel cost of this tour. The unutilized paths are either unviable because of there is not enough recharging facilities to complete the tour for the class of users, or their travel cost is no less that the minimum travel cost for this class of users to complete the tour. Hence, the nonlinear complementarity problem (NCP) form of the multiple classes of users' equilibrium is developed as follow:

$$f_{m,v}^{p,q} \geq 0 \quad \forall p \in P_{m,v}^{q}, m, q, v \tag{7}$$

$$\sum_{a} \delta_{m,v,a}^{OD,p,q} t_a + s_{m,v}^{p,q} + c_{m,v}^{p,q} / w_m^o - T_{m,v}^{q} \geq 0 \quad \forall p \in P_{m,v}^{q}, m, q, v \tag{8}$$

$$f_{m,v}^{p,q} \left(\sum_{a} \delta_{m,v,a}^{OD,p,q} t_a + s_{m,v}^{p,q} + c_{m,v}^{p,q} / w_m^o - T_{m,v}^{q} \right) = 0 \quad \forall p \in P_{m,v}^{q}, m, q, v \tag{9}$$

where constraint (7) describes the non-negativity of path travel flow for each class of users m choosing EV type v to finish the tour q via path p, where $P_{m,v}^{q}$ represents the set of available paths for class m users of tour q choosing EV type v. In constraint (8), $\delta_{m,v,a}^{OD,p,q}$ is an indicator, which equals to 1 if link a is on a path p connecting an OD along a tour q for class m travellers using EV type v, and 0 otherwise; $T_{m,v}^{q}$ stands for the minimum available travel cost for class m users to complete tour q by using vehicle type v; thus, to satisfy equation (9), path flow $f_{m,v}^{p,q} > 0$ only if $\sum_{a} \delta_{m,v,a}^{OD,p,q} t_a + s_{m,v}^{p,q} + c_{m,v}^{p,q} / w_m^o = T_{m,v}^{q}$, which implies that the traffic flow is assigned to paths with minimum travel cost between the same tour origination and destination. Indeed, the NCP formulation has been widely applied in the literature to describe user equilibrium with multi-class or heterogeneous users (Du and Wang, 2014; Farahani et al., 2013; Wang and Du, 2013; Wang and Du, 2016), which can be transformed into a more general variational inequality problem form (Jiang et al., 2016).

The multi-class user equilibrium also needs to satisfy the travel demand conservation equation (10) and the balance relationship (11) between link traffic flow and path traffic flow, which are written as follows:

$$\sum_{p \in P_{m,v}^{q}} f_{m,v}^{p,q} = d_{m,v}^{q} \quad \forall q, m, v \tag{10}$$

$$x_a = \sum_{v \in V} \sum_{m \in M} \sum_{q \in Q} \sum_{p \in P_{m,v}^{q}} \sum_{OD \in \Omega^q} f_{m,v}^{p,q} \delta_{m,v,a}^{OD,p,q} \quad \forall a \tag{11}$$

The travel time function adopted in this paper follows the Bureau of Public Roads (BPR) function, which is expressed in (12) as below:

$$t_a = t_a^0 \left[1 + 0.15 \left(x_a / C_a \right)^4 \right] \quad \forall a \tag{12}$$

Where t_a^0 is the free-flow travel time and C_a is the link capacity.

Note that for a specific EV type, a fixed path and a specific user class with certain anxiety range, the minimum recharging delay $s_{m,v}^{p,q}$ and recharging cost $c_{m,v}^{p,q}$ can be calculated as a constant regardless of link flow. The solution procedure for the multiple classes' UE is rather complicated, which is explained in details in the next section.

3. Solution algorithm

In this section, we present a novel solution algorithm for this multi-type EV charging facilities location problem. Inspired by some recent researches (Regis, 2011; Regis and Shoemaker, 2007) on solution algorithms for derivative-free optimization of expensive black-box objective functions, a heuristic solution algorithm is presented to solve this rather complicated tri-level problem without using derivatives of either objective or constraint functions. In fact, the tri-level model can be treated as an optimization problem with a very expensive black-box objective function, which can be described in the following form:

$$\begin{aligned} &\min \ Z(\mathbf{y}) \\ &s.t. \\ &\mathbf{y} \in \{0,1\} \\ &\sum \mathbf{y} \le \Phi \end{aligned} \tag{13}$$

Where $\mathbf{y}$ represents a construction plan for EV charging stations. Since a government plan on charging station location can impact the consumers' choices on types of EVs and the drivers' routing choice behaviour on network, $Z(\mathbf{y})$ is the expensive black-box objective function, which calculates the upper-level objective function value, i.e., the total social cost, given a specific government construction plan. Apparently, the main input variables of the black-box evaluation in this problem is the government construction plan $\mathbf{y}$, i.e., how and where to locate different types of EV charging facilities; while the output of the black-box is the total social cost of this construction plan. The goal of this problem is to find a feasible construction plan that will lead to the minimum social cost.

Given a specific government construction plan, the middle-level and the lower-level can be solved through conventional methods. Here, a fixed-point iterative method for the middle-level and a method of successive averages (MSA) for the lower-level network equilibrium model are employed, and thus the corresponding social cost can be obtained. The detailed process of how to calculate $Z(\mathbf{y})$ given a known $\mathbf{y}$ is elaborated in the subsection 3.3. As the evaluation of the black-box can be obtained while no information of derivatives is required, solving the original problem is indeed how to search the optimized construction plan through limited evaluations of the expensive black-box function.

The basic idea of the presented solution algorithm is that we use the radial basis function (RBF) surrogate model to approximate the expensive black-box objective function and thus to identify the point to be evaluated for the black-box function in next iteration. The advantage of this method is that only one black-box function evaluation is needed in each iteration, which significantly reduces the computational load because usually the black-box evaluation comprises the majority part of computational effort. The algorithm is designed to obtain good solutions after a relatively small number of iterations. The performance of the solution algorithm is shown in the numerical study section.

3.1 Steps of stochastic RBF-based solution algorithms

The following describes the detailed procedure of stochastic RBF-based solution algorithm:

Step 1: Initialization.

Step1.1 Initial starting points. Find a set of initial starting points $I_0 = \{\mathbf{y}_1, \mathbf{y}_2, ...\mathbf{y}_{n_0}\}$ that contains one feasible plan $\mathbf{y}_1$. The other points do not have to be feasible. For each initial starting point, evaluate the black-box objective function value at this point, i.e., $Z(\mathbf{y}_i)$, and find the best feasible solution $\mathbf{y}_{best}$ among the set I_0. Set the iteration number $n = n_0$ and the set of evaluated points $I_n = I_0$.

Step 1.2: Initial probability of perturbing a dimension of the current best feasible solution when generating random candidate points, denoted by p_{slct}. Initialize the counters for consecutive successes $C_{succ} = 0$ and failures $C_{fail} = 0$.

Step 2: Iteration. *While* the termination condition is not satisfied, do:

Step 2.1: Fit or update the response surface model $S_n(\mathbf{y})$ for the expensive objective function $Z(\mathbf{y})$ by using data points $B_n = \{(\mathbf{y}_i, Z(\mathbf{y}_i)), \mathbf{y}_i \in I_n\}$. Noted that infeasible initial points are also used here to fit the response surface model.

Step 2.2: Randomly generate t candidate feasible points $E_n = \{\mathbf{x}_1, ..., \mathbf{x}_t\}$ for prediction. *For* each $\mathbf{x}_j, j \in 1, ..., t$,

Step 2.2.1: Select dimensions of $\mathbf{y}_{best}$ to perturb. Randomly generate d uniformly distributed numbers $u_1, \ldots, u_d$ in [0,1], where d is the dimension of $\mathbf{y}$. Select the index i of u_i into the set $I_{pert} = \{i \mid u_i < p_{slct}, i \in [1, d]\}$. If $I_{pert} = \varnothing$, uniformly random select an index i from the set $\{1, \ldots, d\}$ and let $I_{pert} = \{i\}$. For each index $i \in I_{pert}$, $\mathbf{x}_j^{(i)} = 1 - \mathbf{y}_{best}^{(i)}$; for index $i \notin I_{pert}$, $\mathbf{x}_j^{(i)} = \mathbf{y}_{best}^{(i)}$.

Step 2.2.2: Make $\mathbf{x}_j$ satisfy the government budget constraint. Calculate the construction cost of $\mathbf{x}_j$, while $\mathbf{x}_j$ do not satisfy the budget constraint, randomly select a dimension $i \in \{1,...,d\}$ where $\mathbf{x}_j^{(i)} = 1$ and let $\mathbf{x}_j^{(i)} = 0$. Calculate the construction cost and check the budget constraint again. Stop and obtain the feasible point $\mathbf{x}_j$ when the constraint is satisfied or repeat this process until the condition is satisfied. *End* this *for* iteration.

Step 2.3: Using the response surface model for the objective function $S_n(\mathbf{y})$ to select the function evaluation point from the generated t candidate feasible points.

Step 2.3.1: Calculate $S_n(\mathbf{x})$ for each candidate plan $\mathbf{x} \in E_n$, also calculate $S^{\min} = \min\{S_n(\mathbf{x}), \mathbf{x} \in E_n\}$ and $S^{\max} = \max\{S_n(\mathbf{x}), \mathbf{x} \in E_n\}$. Then compute score for the response surface criterion, for each $\mathbf{x} \in E_n$, if $S^{\max} \neq S^{\min}$, $V_n^S(\mathbf{x}) = (S_n(\mathbf{x}) - S^{\min}) / (S^{\max} - S^{\min})$; otherwise $V_n^S(\mathbf{x}) = 1$.

Step 2.3.2: Calculate minimum distance from previously evaluated points. For each $\mathbf{x} \in E_n$, this distance is defined as $D_n(\mathbf{x}) = \min_{1 \le i \le n} \|\mathbf{x} - \mathbf{y}_i\|, \mathbf{y}_i \in I_n$. The symbol $\|\cdot\|$ stands for the Euclidean norm. Also calculate $D^{\min} = \min\{D_n(\mathbf{x}), \mathbf{x} \in E_n\}$ and $D^{\max} = \max\{D_n(\mathbf{x}), \mathbf{x} \in E_n\}$. Then compute the score for the distance criterion, for each $\mathbf{x} \in E_n$, the score $V_n^D(\mathbf{x}) = (D^{\max} - D_n(\mathbf{x})) / (D^{\max} - D^{\min})$ if $D^{\max} \neq D^{\min}$; otherwise $V_n^D(\mathbf{x}) = 1$.

Step 2.3.3: Determine the weights for response surface and distance respectively. Set the weight for response surface criterion $w_n^S = \begin{cases} v_{\mathrm{mod}(n-n_0,k)} & \text{if } \mathrm{mod}(n-n_0,k) \neq 0 \\ v_k & \text{otherwise} \end{cases}$ and the weight for the distance criterion $w_n^D = 1 - w_n^S$, where k is an integer and v_i is a series of weights, which satisfy the condition $0 \le v_1 \le ... \le v_k \le 1$. Compute the final weighted score $V_n(\mathbf{x}) = w_n^S V_n^S(\mathbf{x}) + w_n^D V_n^D(\mathbf{x})$ for each $\mathbf{x} \in E_n$ and select the plan $\mathbf{x}^*$ with the minimum weighted score as the next plan to be evaluated in the black box function. Let $\mathbf{y}_{n+1} = \mathbf{x}^*$.

Step 2.4: Evaluate $\mathbf{y}_{n+1}$ by using the black-box objective function, which will be explained in details in the next subsection. Here, we simply assume that we have already known how to solve the black-box objective function.

Step 2.5: Update current best feasible solution $\mathbf{y}_{best} = \mathbf{y}_{n+1}$ and set the counters for consecutive successes $C_{succ} = C_{succ} + 1$, consecutive failures $C_{fail} = 0$ if $\mathbf{y}_{n+1}$ is feasible and $Z(\mathbf{y}_{n+1}) < Z(\mathbf{y}_{best})$; otherwise set $C_{fail} = C_{fail} + 1$ and $C_{succ} = 0$.

Step 2.6: Adjust the perturbing probability p_{slct} via $p_{slct} = 0.5 p_{slct}$ if $C_{fail} \geq C_{fail}^{\max}$, where $C_{fail}^{\max}$ is a given integer parameter, and then set $C_{fail} = 0$. Otherwise if $C_{succ} \geq C_{succ}^{\max}$, adjust the probability $p_{slct} = 2 p_{slct}$ and set $C_{succ} = 0$.

Step 2.7: Update the set of evaluated points $I_{n+1} = I_n \bigcup \{\mathbf{y}_{n+1}\}$ and the iteration index $n = n+1$. *End* the *while* iteration.

Step 3: When the stopping criterion is satisfied, stop and return the current best feasible location plan $\mathbf{y}_{best}$.

In the literature (Regis, 2011; Regis and Shoemaker, 2007), the decision variables are continuous variables, thus the step size parameters are adjusted to control the size of the neighborhood of the current best solution to be checked. While in this paper, the decision variables in the problem is mainly binary rather than continuous, which means the variable value is either be 0 or 1, and therefore, adjusting the step size is insignificant when generating the random candidate points to be predicted in the response surface model. To solve this problem, the perturbing probability p_{slct} is utilized to adjust the average number of dimensions perturbed from the current best solution $\mathbf{y}_{best}$. If the number of consecutive successes is larger than a given constant, p_{slct} is doubled to enlarge the checking area. In case of the number of consecutive failures is larger than a given maximum value, p_{slct} is halved to shrink the checking neighborhood. Then, the value of selected perturbed dimensions of $\mathbf{y}_{best}$ will be directly changed to the other number in $\{0,1\}$. In this way, we can obtain random candidate points much more efficiently.

In Step 1, a set of initial starting points $I_0 = \{\mathbf{y}_1, \mathbf{y}_2, ...\mathbf{y}_{n_0}\}$ that includes one feasible solution $\mathbf{y}_1$ is needed for fitting the initial response surface model. By default, the number of initial starting points $n_0 = d+1$. The feasible solution $\mathbf{y}_1$ can be firstly generated via a random procedure, and then processed via Step 2.2.2 to make it satisfy the budget constraint. If the solution is also evaluated feasible in the black-box function (detailed procedure in the next subsection), this solution can be set as $\mathbf{y}_1$ and be applied to generate all other starting points. Define $\{e_1, ..., e_d\}$ as the natural basis of $\mathbb{R}^d$, the other d starting points $\{\mathbf{y}_2, ...\mathbf{y}_{n_0}\}$ can be defined as $\{|\mathbf{y}_1 - e_1|, ..., |\mathbf{y}_{n_0} - e_d|\}$. This is only one example of the viable methods of generating initial points, while other methods can also be proposed and applied. Please note that it is required that the initial points are affinely independent in fitting the initial response surface model.

In Step 2.3, the evaluation point is selected with minimum weighted score among the set of random generated points. The score is a combined consideration of the two criteria, which is the value of the predicted response surface model value and the minimum distance from previously evaluated points. The second criteria is included because the point with low RBF value is usually near the current best solution $\mathbf{y}_{best}$ and this criteria can promote global search on the feasible region. Besides, the point far away from $\mathbf{y}_{best}$ can also improve the fitting of RBF for the objective function.

3.2 RBF interpolation model

In the presented algorithm, an RBF model as introduced in Powell (1992) and Regis (2011) is employed for the approximation of the expensive black-box objective function, which is equivalent to a form of kriging interpolation like dual kriging method (Cressie, 2015). Kriging is one of the widely used interpolation methods in geostatistics, spatial analysis and computer in the past few decades. It considers the statistical relationships among the measured points when creating the surface, which makes it most appropriate for the data case where spatially correlated distance or directional bias exists. The RBF method is briefly stated below.

In Step 2, given evaluated data points $B_n = \{(\mathbf{y}_i, Z(\mathbf{y}_i)), \mathbf{y}_i \in I_n\}$, the RBF interpolation model is in form of $S_n(\mathbf{y}) = \sum_{i=1}^{n} \varpi_i \phi(\|\mathbf{y} - \mathbf{y}_i\|) + l(\mathbf{y})$, where $\mathbf{y}$ is a d dimensional variable, $\varpi_i, i = 1,\dots,n$ is a series of coefficient to be determined, $\|\cdot\|$ is Euclidean norm, and $l(\mathbf{y})$ is a linear polynomial in d variables to be determined. In kriging interpolation, the function $\phi(r)$ has several available choices, including a linear form ($\phi(r) = r$), a thin plate spline ($\phi(r) = r^2 \log r$), a cubic form ($\phi(r) = r^3$) and so on. Each of them can be used in the RBF interpolation and for simplicity, here the last one $\phi(r) = r^3$ is adopted in $S_n(\mathbf{y})$. Since the points $\mathbf{y}_i$ and their objective function value $Z(\mathbf{y}_i)$ are known, the coefficient vector of cubic RBF interpolation model can be obtained by solving the following equality:

$$\begin{pmatrix} \Phi & L \\ L & 0_{(d+1)\times(d+1)} \end{pmatrix} \begin{pmatrix} \varpi \\ c \end{pmatrix} = \begin{pmatrix} Z \\ 0_{d+1} \end{pmatrix} \tag{14}$$

Where Φ is an $n \times n$ matrix and $\Phi(i,j) = \phi(\|\mathbf{y}_i - \mathbf{y}_j\|), i, j = 1,\dots,n$, L is defined as $\begin{pmatrix} 1 & \mathbf{y}_1^T \\ \vdots & \vdots \\ 1 & \mathbf{y}_n^T \end{pmatrix}$ and $Z = (Z(\mathbf{y}_1),\dots,Z(\mathbf{y}_n))^T$. The coefficient vector to be determined consists of $\varpi = (\varpi_1,\dots,\varpi_n)^T$ and $c = (c_1,\dots,c_{d+1})^T$; the latter indeed contains the coefficients of the linear polynomial function $l(\mathbf{y})$. The coefficient vector $(\varpi \quad c)^T$ can be calculated if and only if $\mathrm{rank}(L) = d + 1$ (Powell, 1992). This is also the reason why the initial starting points are required to be affinely independent in the initialization step of the solution algorithm.

3.3 Evaluation of the black-box function

In this section, the evaluation of the expensive black-box function $Z(\mathbf{y})$ is presented, which is applied in both Step 1.1 and Step 2.4 of the presented stochastic RBF-based algorithm. It is equivalent to solving a combination of the middle-level constraints and the lower-level user equilibrium to obtain the travel system performance index, i.e., the objective function of the original problem, given a known EV charging station location plan $\mathbf{y}$. In fact, the evaluation process of the black-box objective function is quite complicated and consumes dominant computational time in the whole presented solution algorithm.

There are two main steps included in the evaluation of the black-box objective function. First, an MSA solution method for the restricted user equilibrium is stated, through which the network equilibrium can be calculated for a specific EV charging station plan $\mathbf{y}$ and demand $d_{m,v}^{q}$. Second, a fixed-point iteration method is presented to solve the users' selection between different EV types by incorporating the MSA solution process as the sub-problem. Details of the evaluating procedure are stated below.

3.3.1 MSA solution method for the lower-level user equilibrium

Given a known EV charging station location plan $\mathbf{y}$ and a known customers' demand $d_{m,v}^{q}$ of different EV types, an MSA method is employed in this subsection to solve the tour-based network equilibrium model. We assume that the recharging delay time function is linear, the maximum recharging energy on a specific wireless recharging link is a fixed value and the energy consumption is irrelevant of traffic flow. These assumptions are used to simplify the problem and may compromise the model description of realistic practice, which are indeed worthy of special studies in the future. For example, EV energy recharged on a wireless recharging link is actually related to the driving time on this link according to the researches of Jang et al. (2015), Ko et al. (2015) and Chen et al. (2016). However, to ensure the major topic of this study can be focused and addressed and the model solution is more tractable, we adopt the simplified assumptions in this paper and leave the extended and more practical assumptions to be investigated in the future studies. When the location plan $\mathbf{y}$ is known, the minimum recharging time is actually fixed and unique for specific class m travelers using vehicle type v traversing a tour path p. In addition, the BPR link travel time function is also strictly increasing. According to the work of Dafermos (1971, 1972), the multi-class traffic assignment problem can be reformulated as a nonseparable single class network equilibrium problem. The nonseparable problem, when the Jacobian matrix of travel cost function is symmetric, can be reduced to a minimization problem. In the developed model, it is obvious that one class travellers using a type of EVs on one link has the same impact on another class of users as much as the latter class on this link impact the former one, which means the Jacobian matrix is symmetric. Hence, the equilibrium link flow is unique for this tour-based network equilibrium model.

Once the EV charging station location plan is given, all the paths for any specific class m travelers using vehicle type v can be enumerated. In this way, the lower-level network user equilibrium problem can be directly solved by applying conventional solution methods for UE, such as Frank-Wolfe algorithm and MSA method. In this subsection, the MSA is used to solve the network user equilibrium. However, the path enumeration considering EV charging activity is complicated and takes considerable time in the computational process. Here, the method of restricted version of UE, which is presented in He et al. (2014), is applied in solving the lower-level problem. This method avoids the tedious path enumeration procedure while still guarantees the exact solution of the original UE. The basic idea of this method is that, rather than enumerating all the paths, a sub-problem is invented to generate a shortest path in each iteration, which is stored in a set of shortest paths, and then the original user equilibrium is solved with all these generated shortest paths. The iterative process terminates when the new generated path is no shorter than all the paths stored in the subset for the same user class. The key point of this method is to develop the shortest-path-finding sub-problem for each user class and specific situation. In this section, two shortest-path-finding sub-problems for wireless and plug-in charging EVs are developed below, respectively. The first one of the two sub-problems is a mixed-integer linear programming (MILP) and the second one is nonlinear, which can be further transformed into equivalent MILP by applying reformulation-linearization technique (RLT) (Sherali and Adams, 1999). Thus, both of the two problems can be directly solved by conventional methods for MILP or using commercial solvers like CPLEX and Gurobi.

Given the EV charging station location plan and the current link flow solution ($\ldots \mu_a \ldots$), the sub-problem, i.e., the shortest usable tour path finding problem for the restricted lower level network equilibrium problem can be formulated as follows for each combination of user class m, EV type v and tour q. For wireless charging EV, the shortest-path-finding problem is developed as below:

$$\min \sum_{\omega\in\Omega^q}\sum_{a\in A} t_a(\mu_a)x_a^{\omega} + \sum_{\omega\in\Omega^q}\sum_{i\in N_2^c} K_{i,m}^{\omega,wlss} + \left(\sum_{\omega\in\Omega^q}\sum_{i\in N_2^c} R_{i,m}^{\omega,wlss} + \sum_{\omega\in\Omega^q}\sum_{a\in A_1^c} R_{a,m}^{\omega,wlsd}\right)/w_m^o \tag{15}$$

s.t.

$$\Delta\mathbf{x}^{\omega} = \mathbf{E}^{\omega} \quad \forall\omega\in\Omega^q \tag{16}$$

$$S_{j,m,v}^{\omega} - S_{i,m,v}^{\omega} + e_a - F_{j,m,v}^{\omega} - I_{a,m}^{\omega} = \varepsilon_a^{\omega} \quad \forall\omega\in\Omega^q, (i,j)=a\in A \tag{17}$$

$$-M(1-x_a^{\omega}) \le \varepsilon_a^{\omega} \le M(1-x_a^{\omega}) \quad \forall a\in A, \omega\in\Omega^q \tag{18}$$

$$0 \le F_{i,m,v}^{\omega} \le B_i \quad \forall\omega\in\Omega^q, i\in N \tag{19}$$

$$0 \le S_{i,m,v}^{\omega} \le L_v \quad \forall\omega\in\Omega^q, i\in N \tag{20}$$

$$\zeta_{a,m}^{\omega} \ge I_{a,m}^{\omega} / I_a^0 \quad \forall a\in A_1^c, \omega\in\Omega^q \tag{21}$$

$$\zeta_{a,m}^{\omega} \le M I_{a,m}^{\omega} \quad \forall a\in A_1^c, \omega\in\Omega^q \tag{22}$$

$$\zeta_{a,m}^{\omega} \in \{0,1\} \quad \forall a\in A_1^c, \omega\in\Omega^q \tag{23}$$

$$0 \le I_{a,m}^{\omega} \le I_a^0 \quad \forall a\in A, \omega\in\Omega^q \tag{24}$$

$$S^{\omega}_{O(\omega),m,v} = S^{0}_{m,v} \quad \forall \omega \in \Omega^q, O(\omega) = O(q) \tag{25}$$

$$S^{\omega_1}_{D(\omega_1),m,v} = S^{\omega_2}_{O(\omega_2),m,v} \quad \forall \omega_1 \in \Omega^q, \omega_2 \in \Omega^q,\ D(\omega_1) = O(\omega_2) \tag{26}$$

$$\eta^{\omega}_{i,m,v} \geq F^{\omega}_{i,m,v} / B^{\max} \quad \forall \omega \in \Omega^q, i \in N^c_2, i \neq D(\omega), O(\omega) \tag{27}$$

$$\eta^{\omega}_{i,m,v} \in \{0,1\} \quad \forall \omega \in \Omega^q, i \in N^c_2, i \neq D(\omega), O(\omega) \tag{28}$$

$$x^{\omega}_a \in \{0,1\} \quad \forall a \in A, \omega \in \Omega^q \tag{29}$$

$$R^{\omega,wlss}_{i,m} = r^{wlss}_i F^{\omega}_{i,m,v} \quad \forall \omega \in \Omega^q, i \in N^c_2 \tag{30}$$

$$K^{\omega,wlss}_{i,m} = \alpha^s_i \eta^{\omega}_{i,m,v} + \alpha^{wlss}_i F^{\omega}_{i,m,v} \quad \forall \omega \in \Omega^q, i \in N^c_2, i \neq D(\omega), O(\omega) \tag{31}$$

$$K^{\omega,wlss}_{D(\omega),m} \geq \alpha^{wlss}_{D(\omega)} F^{\omega}_{D(\omega),m,v} - T^q_{D(\omega)} \quad \forall \omega \in \Omega^q, D(\omega) \neq D(q) \tag{32}$$

$$K^{\omega,wlss}_{D(\omega),m} \geq 0 \quad \forall \omega \in \Omega^q, D(\omega) \neq D(q) \tag{33}$$

$$R^{\omega,wlsd}_{a,m} = r^{wlsd}_a I^{\omega}_{a,m} \quad \forall a \in A^c_1, \omega \in \Omega^q \tag{34}$$

$$S^{\omega}_{i,m,v} - e_a \geq -M(1 - x^{\omega}_a) - M\zeta^{\omega}_{a,m} + G_m L_v \quad \forall (i,j) = a \in A^c_1, \omega \in \Omega^q \tag{35}$$

$$S^{\omega}_{i,m,v} - e_a \geq -M(1 - x^{\omega}_a) + G_m L_v \quad \forall (i,j) = a \notin A^c_1, \omega \in \Omega^q \tag{36}$$

The objective is to minimize the tour path travel cost, including the pure travel time under this traffic flow $\sum_{\omega \in \Omega^q} \sum_{a \in A} t_a(\mu_a) x^{\omega}_a$, recharging fee $\left(\sum_{\omega \in \Omega^q} \sum_{i \in N^c_2} R^{\omega,wlss}_{i,m} + \sum_{\omega \in \Omega^q} \sum_{a \in A^c_1} R^{\omega,wlsd}_{a,m} \right) / w^o_m$ measured in terms of time and recharging delay because of wireless static recharging $\sum_{\omega \in \Omega^q} \sum_{i \in N^c_2} K^{\omega,wlss}_{i,m}$, wherein binary variable x^{ω}_a indicates whether or not link a is on the current shortest useable path of an OD pair ω on tour q, Ω^q is the set of OD pairs included in tour q, $R^{\omega,wlss}_{i,m}$ is the stationary wireless recharging cost at node i of class m drivers choosing wireless charging EV traveling between an OD pair ω, $R^{\omega,wlsd}_{a,m}$ is the dynamic recharging cost on link a of class m drivers choosing wireless charging EV traveling between an OD pair ω, and $K^{\omega,wlss}_{i,m}$ defines the delay time of stationary wireless charging behavior at node i of class m drivers choosing wireless charging EV traveling between an OD pair ω. N^c_2 denotes the set of nodes where stationary wireless charging stations are built in the current location plan and A^c_1 is the present set of links with dynamic wireless charging lanes.

Constraint (16) describes the traffic flow conservation on the whole network, wherein $\mathbf{x}^{\omega} = [x^{\omega}_a]$ is a column vector with a length of $|A|$. Δ is the node-link incidence matrix with a size of $|N| \times |A|$ and $\Delta = \left[\delta^n_a\right]$, where $\delta^n_a = 1$ if node n lies at the entrance of link a,

$\delta_a^n = -1$ if node n lies at the exit of link a, and $\delta_a^n = 0$ otherwise. A column vector $\mathbf{E}^{\omega}$ is defined with a length of $|N|$ between each OD pair ω, wherein the elements equals to 1 at the origin node, -1 at the destination node and 0 otherwise. Constraints (17) and (18) ensure the conservation of energy, which is an equivalent relationship between the pure consumed energy and the loss of EV battery charge on any utilized link, while unrestricted for any unutilized link. For each link $(i, j) = a \in A$, $S_{i,m,v}^{\omega}$ stands for the status of battery power at node i of class m drivers choosing EV type v traveling between an OD pair ω; if node i is a recharging station, $S_{i,m,v}^{\omega}$ refers to the status of battery power after recharging. e_a is the amount of electricity consumed on the link. $F_{i,m,v}^{\omega}$ is the amount of electricity charged at node i and $I_{a,m}^{\omega}$ represents the amount of electricity charged when driving on link a. ε_a^{ω} is a variable, which equals to zero if link a is on the currently shortest path, otherwise ε_a^{ω} is unrestricted. M in constraint (18) is a large enough positive number. Constraints (19), (20) and (24) are the bound constraints for the amount of electricity charged at node i $F_{i,m,v}^{\omega}$, state of EV battery charge at node i $S_{i,m,v}^{\omega}$ and the amount of electricity charged by using wireless charging lane on link a $I_{a,m}^{\omega}$, respectively, where B_i is the upper bound of electricity that an EV can charge at node i, L_v is the battery size of an EV of type v, and I_a^0 represents the upper bound of electricity that a wireless charging EV can charge on link a. Constraints (21) -(23) are used to indicate whether a wireless recharging lane on link a is employed, binary variable $\zeta_{a,m}^{\omega} = 1$ if this lane is used by the specific user class and 0 otherwise. Constraint (25) describes the state of charge of EV battery at starting node of the tour and constraint (26) ensures that there is no loss of charge of EV battery between two consecutive trips. $O(\cdot)$ and $D(\cdot)$ represents the origin point and the destination point of a trip or a tour, respectively. $S_{m,v}^0$ is the starting status of battery power of class m drivers choosing EV type v. Constraints (27) and (28) indicate whether a static wireless charging station at note i is employed, where $\eta_{i,m,v}^{\omega} = 1$ if the wireless charging station is used and 0 otherwise; $B^{\max} = \max_{i \in N}(B_i)$. The binary variable x_a^{ω} in constraint (29) is the key variable in this sub-problem, which is used to indicate the shortest path of the tour under this current traffic flow situation. Static wireless charging cost and dynamic wireless charging cost are calculated in constraints (30) and (34) respectively. Here, it is assumed that the charging fee is a linear function of the amount of recharging electricity. r_i^{wlss} is the unit price of stationary wireless charging at node i and r_a^{wlsd} is the unit price of dynamic wireless charging on link a. Since the static wireless charging also results in travel delay for the tour, constraints (31)-(33) are developed to calculate the delay time $K_{i,m}^{\omega,wlss}$, which is also a linear function of the amount of recharging electricity minus the planned stopping time at this node of the tour. α_i^s represents the fixed time for stopping and starting an EV at node i for recharging and α_i^{wlss} defines the time for wireless charging EV recharging a unit amount of electricity at node i. $T^{q}_{D(\omega)}$ refers to the dwelling time of tour q travelers at node $D(\omega)$. Constraints (35) and (36) describe the impact of range anxiety of class m user on the EV battery state of charge in the cases of recharging on link a and not recharging on link a, respectively, where G_m refers to the buffer range rate of class m drivers. It is clear that the shortest-path-finding sub-problem for wireless charging EV is an MILP, which can be solved through various commercial solvers, such as CPLEX and Gurobi.

For plug-in charging EV, the shortest-path-finding problem is similar to the sub-problem for wireless charging EV except for those constraints related to the employment of different levels of charging stations at one node. The sub-problem is developed as following:

$$\min \sum_{\omega\in\Omega^q}\sum_{a\in A} t_a(\mu_a)x_a^{\omega} + \sum_{\omega\in\Omega^q}\sum_{i\in N_1^c} K_{i,m}^{\omega,plu} + \left(\sum_{\omega\in\Omega^q}\sum_{i\in N_1^c} R_{i,m}^{\omega,plu}\right) / w_m^o \tag{37}$$

s.t.

(16), (18)-(20), (25), (26), (29)

$$S_{j,m,v}^{\omega} - S_{i,m,v}^{\omega} + e_a - F_{j,m,v}^{\omega} = \varepsilon_a^{\omega} \quad \forall \omega\in\Omega^q, (i,j)=a\in A \tag{38}$$

$$\eta_{i,m,v}^{\omega} \geq F_{i,m,v}^{\omega} / B^{\max} \quad \forall \omega\in\Omega^q, i\in N_1^c, i\neq D(\omega), O(\omega) \tag{39}$$

$$\eta_{i,m,v}^{\omega} \in \{0,1\} \quad \forall \omega\in\Omega^q, i\in N_1^c, i\neq D(\omega), O(\omega) \tag{40}$$

$$\sum_{\psi\in\Psi} \xi_{\psi,i,m}^{\omega} = \eta_{i,m,v}^{\omega} \quad \forall \omega\in\Omega^q, i\in N_1^c, i\neq D(\omega), O(\omega) \tag{41}$$

$$\xi_{\psi,i,m}^{\omega} \in \{0,1\} \quad \forall \psi\in\Psi, \omega\in\Omega^q, i\in N_1^c, i\neq D(q), O(q) \tag{42}$$

$$R_{i,m}^{\omega,plu} = \sum_{\psi\in\Psi} r_i^{plu} F_{i,m,v}^{\omega} \xi_{\psi,i,m}^{\omega} \quad \forall \omega\in\Omega^q, i\in N_1^c, i\neq D(q), O(q) \tag{43}$$

$$K_{i,m}^{\omega,plu} = \alpha_i^s \eta_{i,m,v}^{\omega} + \sum_{\psi\in\Psi} \alpha_{\psi,i}^{plu} F_{i,m,v}^{\omega} \xi_{\psi,i,m}^{\omega} \quad \forall \omega\in\Omega^q, i\in N_1^c, i\neq D(\omega), O(\omega) \tag{44}$$

$$K_{D(\omega),m}^{\omega,plu} \geq \sum_{\psi\in\Psi} \alpha_{\psi,D(\omega)}^{plu} F_{D(\omega),m,v}^{\omega} \xi_{\psi,D(\omega),m}^{\omega} - T_{D(\omega)}^{q} \quad \forall \omega\in\Omega^q, D(\omega)\in N_1^c, D(\omega)\neq D(q) \tag{45}$$

$$K_{D(\omega),m}^{\omega,plu} \geq 0 \quad \forall \omega\in\Omega^q, D(\omega)\in N_1^c, D(\omega)\neq D(q) \tag{46}$$

$$S_{i,m,v}^{\omega} - e_a \geq -M(1-x_a^{\omega}) + G_m L_v \quad \forall (i,j)=a\in A, \omega\in\Omega^q \tag{47}$$

Here, $K_{i,m}^{\omega,plu}$ represents the delay time of recharging behavior at node i of class m drivers choosing plug-in charging EV traveling between an OD pair ω and $R_{i,m}^{\omega,plu}$ is the recharging cost; r_i^{plu} is the price of plug-in charging at node i; binary variable $\xi_{\psi,i,m}^{\omega}$ indicates whether or not class m travelers using plug-in charger of type ψ at node i; $\alpha_{\psi,i}^{plu}$ is the recharging time for plug-in EV charging a unit amount of electricity through type ψ charger at node i.

Constraint (38) describes the conservation of energy. Compared to constraint (17), the term of electricity recharged on wireless charging link is removed from this constraint. Constraints (39) and (40) state whether plug-in charging EV of user class m recharge at node i, which belongs to the set of plug-in charging station locations N_1^c. Constraints (41) and (42) introduce a new variable to indicate whether a level $\psi \in \Psi$ charging facility is utilized by class m users, where Ψ is the set of charging facility levels that the given government location plan is planning to construct. Constraint (43) calculates the recharging fee, which is also a linear function of the amount of electricity recharged. The recharging fee is transferred into equivalent time cost in the objective function of the sub-problem. Delay time because of plug-in recharging behavior is calculated through constraints (44)-(46). The last constraint (47) describes the effect of range anxiety on state of EV battery charge in this plug-in charging EV case. However, since constraints (43)-(45) contains a common bilinear term $F_{i,m,v}^{\omega}\xi_{\psi,i,m}^{\omega}$, these constraints are nonlinear and lead to the nonconvex property of the whole sub-problem. If the sub-problem is directly solved by conventional methods for nonlinear problem, the solution path may not be the shortest path under the current traffic flow situation. To guarantee the path solved be shortest path, the RLT (Sherali and Adams, 1999) is applied here to facilitate the transformation of the nonconvex sub-problem into an equivalent MILP. The latter problem can be directly solved by commercial solvers and the solution is guaranteed to be global optimal, that is, the shortest path in the current situation.

To linearize the bilinear term, for each $\psi \in \Psi, \omega \in \Omega^q, i \in N_1^c, i \neq D(q), O(q)$, let $\theta_{\psi,i,m}^{\omega} = F_{i,m,v}^{\omega}\xi_{\psi,i,m}^{\omega}$. Thus plug-in charging cost can be rewritten as:

$$R_{i,m}^{\omega,plu} = \sum_{\psi \in \Psi} r_i^{plu}\theta_{\psi,i,m}^{\omega} \quad \forall \omega \in \Omega^q, i \in N_1^c, i \neq D(q), O(q) \tag{48}$$

Delay time because of plug-in recharging behavior can be rewritten as:

$$K_{i,m}^{\omega,plu} = \alpha_i^s \eta_{i,m,v}^{\omega} + \sum_{\psi \in \Psi} \alpha_{\psi,i}^{plu}\theta_{\psi,i,m}^{\omega} \quad \forall \omega \in \Omega^q, i \in N_1^c, i \neq D(\omega), O(\omega) \tag{49}$$

$$K_{D(\omega),m}^{\omega,plu} \geq \sum_{\psi \in \Psi} \alpha_{\psi,D(\omega)}^{plu}\theta_{\psi,D(\omega),m}^{\omega} - T_{D(\omega)}^{q} \quad \forall \omega \in \Omega^q, D(\omega) \in N_1^c, D(\omega) \neq D(q) \tag{50}$$

Following the rules of RLT, $\theta_{\psi,i,m}^{\omega} = F_{i,m,v}^{\omega}\xi_{\psi,i,m}^{\omega}$ is equivalent to the following linear constraints:

$$\begin{aligned}
&\theta_{\psi,i,m}^{\omega} \geq 0 \\
&\theta_{\psi,i,m}^{\omega} - \xi_{\psi,i,m}^{\omega} B_i \leq 0 \\
&\theta_{\psi,i,m}^{\omega} - F_{i,m,v}^{\omega} \leq 0 \\
&\theta_{\psi,i,m}^{\omega} - F_{i,m,v}^{\omega} + B_i - \xi_{\psi,i,m}^{\omega} B_i \geq 0
\end{aligned} \tag{51}$$

To prove the equivalence between these two, we can separately let $\xi_{\psi,i,m}^{\omega}$ equal to 1 or 0 and plug it into (51). In this way, we have,

$$\xi^{\omega}_{\psi,i,m} = 1 \Leftrightarrow \left\{ \begin{array}{l} \theta^{\omega}_{\psi,i,m} \geq 0 \\ \theta^{\omega}_{\psi,i,m} \leq B_i \\ \theta^{\omega}_{\psi,i,m} \leq F^{\omega}_{i,m,v} \\ \theta^{\omega}_{\psi,i,m} \geq F^{\omega}_{i,m,v} \end{array} \right\} \Leftrightarrow \theta^{\omega}_{\psi,i,m} = F^{\omega}_{i,m,v} \tag{52}$$

$$\xi^{\omega}_{\psi,i,m} = 0 \Leftrightarrow \left\{ \begin{array}{l} \theta^{\omega}_{\psi,i,m} \geq 0 \\ \theta^{\omega}_{\psi,i,m} \leq 0 \\ \theta^{\omega}_{\psi,i,m} \leq F^{\omega}_{i,m,v} \\ \theta^{\omega}_{\psi,i,m} + (B_i - F^{\omega}_{i,m,v}) \geq 0 \end{array} \right\} \Leftrightarrow \theta^{\omega}_{\psi,i,m} = 0 \tag{53}$$

This proves the equivalent between the bilinear term $\theta^{\omega}_{\psi,i,m} = F^{\omega}_{i,m,v}\xi^{\omega}_{\psi,i,m}$ and the set of linear constraints (51). So far, by applying RLT technique, the shortest-path-finding sub-problem for plug-in charging EV can be transferred into the following equivalent MILP form:

$$\min \sum_{\omega\in\Omega^q} \sum_{a\in A} t_a(\mu_a) x^{\omega}_a + \sum_{\omega\in\Omega^q} \sum_{i\in N_1^c} K^{\omega,plu}_{i,m} + \left(\sum_{\omega\in\Omega^q} \sum_{i\in N_1^c} R^{\omega,plu}_{i,m} \right) / w^{o}_{m} \tag{37}$$

s.t.

(16), (18)-(20), (25), (26), (29)

(38)-(42), (46)-(51).

The steps of the MSA method for the restricted user equilibrium is stated below:

Step 1:	Initialization. Set flag=1, iter=0, set of shortest path $P = \varnothing$.
Step 2:	**while** flag>0 Set iter=iter+1 Step 2.1: **if** iter>1 Solve the multiclass restricted user equilibrium using current set of shortest paths found for each user class and EV type on each tour: Step 2.1.1: Set iteration index $n = 0$, all link flow equal to 0. Find the path with minimum travel cost and assign all travel demand on the path. Obtain the current link flow μ^0_a. **while** err>tolerance Step 2.1.2: Calculate the link travel time and assign all travel demand on the shortest path to obtain the feasible direction of link flow χ^n_a. Step 2.1.3: Update current link flow $\mu^{n+1}_a = \mu^n_a + (\chi^n_a - \mu^n_a)/n$ for all links and calculate err. Let $n = n+1$. **end**. Step 2.1.4: Return the current link flow and the minimum path travel cost. **end**.
Step 3:	Set flag=0

for each combination of user class and EV type
  Solve the shortest-path-finding sub-problem directly.
  if the travel cost of the new shortest path solved is smaller than the current minimum travel cost
    Add this path to the set of shortest path P
    Set flag=1
  end
end
end

Step 4:	Return the current link flow as the equilibrium link flow.

Here, the words *'travel cost'* includes pure travel time, the delayed time due to recharging behavior, and the unit wage weighted recharging fee.

3.3.2 Fixed-point iteration method for the EV type selection

Because the users' selection between different EV types in the middle-level is both related to the location of EV charging station plan in the upper-level and the users' equilibrium tour travel cost in the lower-level, hence, solving this problem is very complicated. Since in section 3.3.1 the solution method for the lower-level is given, here, it is incorporated in the iterations of fixed-point method in this sub-section as a sub-problem to assist calculating of users' probability of choosing different EV types. In this section, the goal is to solve the road user's choice probability of multiple EV types, supposing the location plan of multiple EV charging stations are given.

The solution algorithm for this problem is inspired by the classical fixed-point iteration method for solving nonlinear equations. The basic idea of this numerical method is to, first convert the equations into the form of $x = f(x)$, which is a fixed-point of x; second, using a starting point x_0 to calculate $x_1 = f(x_0)$ and then repeat this process until the stopping condition is satisfied. In this problem, the probability λ_v^q is treated as the fixed-point, while the lower-level user equilibrium traffic assignment (7)-(12) and the calculation of equations (4)-(6) are treated as the function $f(x)$. In details, the procedure of the fixed-point iteration method for the EV type selection can be stated as follows:

Step 1: Initialize a starting probability $\boldsymbol{\lambda}_0$ for each type of EV (e.g. both from 0.5 for the two types). Set iteration number $n = 1$.

Step 2: Use equation (6) and the current $\boldsymbol{\lambda}_n$ to calculate the travel demand $d_{m,v}^q$ for each user class m of tour q choosing EV type v. Plug the starting travel demand into the lower-level user equilibrium and solve the user equilibrium by using the presented MSA algorithm in the 3.3.1.

Step 3: Use the travel cost from the lower-level problem and equations (4)-(5) to calculate the new probability $\boldsymbol{\lambda}_{n+1}$.

Step 4: Check the convergence of the sequence (λ_n). Go to step 5 if it converges, otherwise let $n = n+1$ and go to step 2.

Step 5: Return the probability $\boldsymbol{\lambda}_n$ as the final solution of customers' choice of different EV types, and the current equilibrium link flow from the lower-level MSA solution result.

So far, with the given the specific EV charging station location plan, the key part of the black-box problem is solved, that is, the customers' choice of different EV types in the middle-level and the resultant user equilibrium traffic flow can be obtained. Then these results can be used to calculate the objective function value of (1), which is returned as the value of the black-box objective function $Z(\mathbf{y})$ and utilized in the RBF-based solution algorithm.

Note that the solution of the fixed-point method is related to the initial starting point, and different starting points can be tried if the (λ_n) sequence does not converge. From the testing results of our numerical examples, starting from the point 0.5 for each type can lead to the final solution in almost every cases. In the worst case, where the probability solution cannot be calculated, the black-box problem is marked as infeasible and the current best location plan in the RBF based solution algorithm will not be updated, but the whole algorithm can still continue and search for a better location plan. This indicates one of the prominent merits of the RBF-based solution algorithm, that is, it can tolerate fault in the solution process, which is very important especially for computer-aided calculation or simulation.

4. Numerical examples

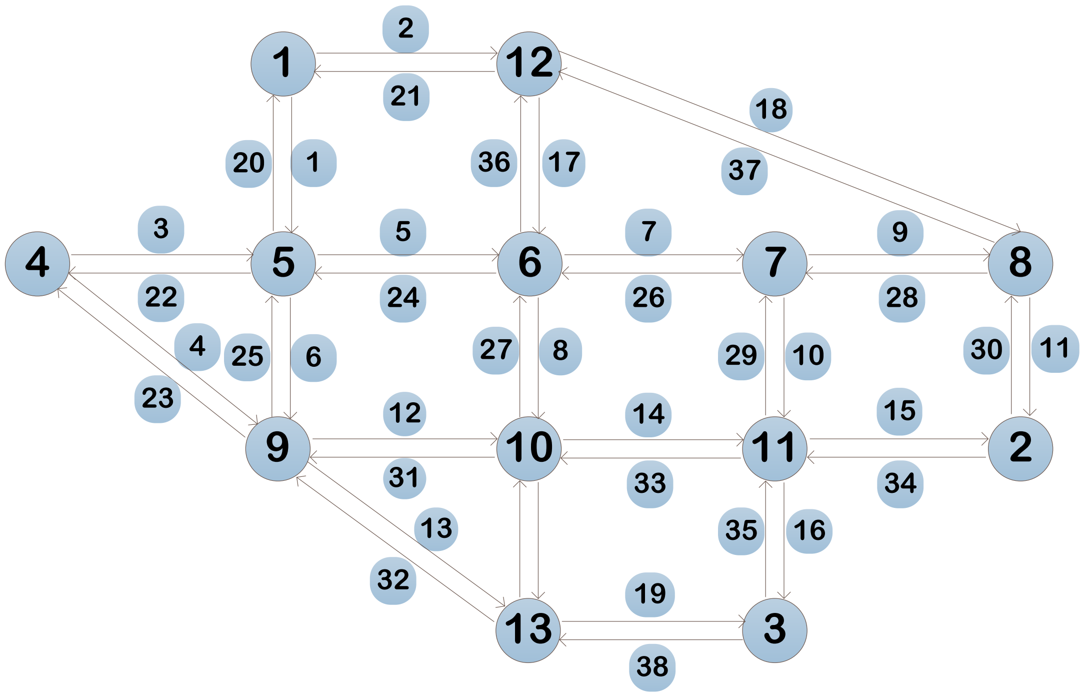

Figure 2 The Nguyen-Dupuis network.

In this section, numerical examples are conducted to test the validity of the proposed model and performance of solution algorithms. As our major objective in this paper is to propose a mathematical model and solution algorithm for locating various types of EV charging stations, a small and a larger network are used in this section to illustrate the concept, application method and performance of the model and solution algorithm. In this section, first, we show the result of the small network and then test the impact of different government budget on locating charging stations. Second, solution performance of the presented solution algorithm is demonstrated. What's more, result of the presented model is compared with that of the model without the middle-level programing. Finally, results of the larger network are reported and analyzed.

4.1. The Nguyen-Dupuis network

The following set of tests are conducted on the Nguyen-Dupuis network (Nguyen and Dupuis, 1984) as the benchmark example. In the literature, this network only contains one direction of roads, i.e., there is no path back to the starting point; however, as the proposed model is tour-based and it is ideal that all the testing tours could end at their starting nodes (traveler commutes from home in the morning and back home in the evening), the number of links on the network is doubled by considering two directions of roads in the new network, as is shown in Figure 1. All the nodes and links are labeled with an index number. In total, this network contains 13 nodes, which indicate 13 intersections, and 38 links, which represent both two directions of 19 roads. All the nodes are available for locating all types of charging stations, including both wireless and traditional wired charging stations. All the links are available for constructing a special wireless charging lane. The two ways of each road will be considered at the same time because one road is usually treated as a whole in practice.

Certainly, the presented model and solution algorithm do not require it to be so, and the two directions of the road can be considered separately.

Table 1 lists the link input parameters for the Nguyen-Dupuis network, including link free flow travel time, link capacity and length, and each pair of links shares the same settings. Assume there are two tours in total for the test. The demand of each tour, the OD pairs and dwelling time at each destination node is listed in Table 2. For each tour, there are two choices of EV types as mentioned in the above text and three classes of road users with the same share of travel demand. We assume the three classes of travelers are frequent, average and modest travelers. The initial states of charge of their EVs are 1.0, 0.8 and 0.6 of the EV battery capacity, which is set as 24 kWh. The buffer ranges of the three classes are 0.2, 0.1 and 0 of the EV battery capacity, respectively. The hourly wage rate of each class is \$80, \$40 and \$15 and the annual income of each class is set equal to the unit income$\times 40 \times 52$. The coefficients of travel cost in the middle-level vehicle choice model in this study are set as -0.0375, -0.0625 and -0.0875, based on the suggested coefficients in Nie et al. (2016), i.e., -0.3, -0.5 and -0.7 for each consumer class, multiplied by a logit model parameter 0.125, representing the travel cost perception variations. The purchasing price G_v, which contains vehicle cost and charging equipment cost, is set as \$40 thousand and \$31 thousand (Nie et al., 2016) for wireless and plug-in charging EVs respectively. The life expectance of each type of EV is assumed to be 10 years. The coefficient of EV purchasing cost in the vehicle choice model is set as -1 and it is assumed that there is no other tour related cost thus β_q is set as 0. The construction cost for the levels 1, 2 and 3 plug-in charging stations are \$1.19, \$4.25 and \$8.5 million respectively (He et al., 2015), while the construction cost of the wireless charging is assumed to be \$6 million for wireless static charging and \$4 million per mile for dynamic charging on link (Fuller, 2016). Set the fixed delay time for charging $\alpha_i^s = 5\text{min}$, and $\alpha_i^{plu} = 41.76\text{min}, 10\text{min and } 0.76\text{min}$ respectively for level 1, 2 and 3 (He et al., 2015). The recharging fee for each level is \$0.08, \$0.2 and \$0.3 per kWh. The delay time and recharging fee for wireless static charging are assumed to be the same with level 2 charging; the recharging cost is set as \$0.5 per kWh and there is no delay time for wireless dynamic charging. In the objective function, the inconvenience cost for each unfinished trip of a tour is equal to 1000 min delay and weighted factor of EV trip failure cost χ is set equal to 0.5.

The experiments are performed on a Windows platform with a 64-bit Windows 10 Pro operating system, an Intel(R) Xeon(R) CPU E5 2609 0 @2.40 GHz,2.40 GHz (two processors) and 32 GB RAM. The free toolbox YALMIP R20150908 (Löfberg, 2004) together with MATLAB R2013b is adopted to model the example. The commercial optimization solver Gurobi optimizer v6.0.5 (Gurobi Optimization, 2016) is used as an external solver of YALMIP to solve all MIP problems to their global optimal solutions.

Table 1

Link free-flow travel time and link capacity for the test network.

Link pairs	Free-flow travel time (min)	Capacity (veh/h)	Length (mile)	Link pairs	Free-flow travel time (min)	Capacity (veh/h)	Length (mile)
1, 20	7	300	8.75	11, 30	9	500	11.25
2, 21	9	200	11.25	12, 31	10	550	12.5

3, 22	9	200	11.25	13, 32	9	200	11.25
4, 23	12	200	15	14, 33	6	400	7.5
5, 24	3	350	3.75	15, 34	9	300	11.25
6, 25	9	400	11.25	16, 35	8	300	10
7, 26	5	500	6.25	17, 36	7	200	8.75
8, 27	13	250	16.25	18, 37	14	300	17.5
9, 28	5	250	6.25	19, 38	11	200	13.75
10, 29	9	300	11.25				

Table 2

Tour input parameters for the test network.

Tour 1		Tour 2	
Demand (veh/h)	100	Demand (veh/h)	50
OD pairs	Dwelling time (min)	OD pairs	Dwelling time (min)
(1,6)	30	(4,7)	10
(6,3)	5	(7,2)	5
(3,1)		(2,4)	

4.1.1 Result of the Nguyen-Dupuis network

Given budget as 150 million, the location plan we obtained from the presented solution algorithm is shown in Table 3. The result locates five level 3 stations for plug-in recharging, as well as two wireless charging lanes for dynamic recharging. The objective function value, i.e. the social welfare, and the probabilities of customers' choice of different types of EVs are reported in Table 4. The objective value is 6773.80 with no missed tour in this test example. Table 5 shows the equilibrium traffic flow if the obtained EV charging station location plan is applied. Figure 3 compares the minimum travel costs, including travel time, delay time due to recharging and wage weighted recharging cost, between wireless and plug-in charging EVs for three different classes of travelers of each tour. It shows that, the Class 1 and 2 travelers of tour 1 choosing wireless charging EV will have a smaller travel cost, while the Class 3 travelers of tour 1 and all the tour 2 travelers will not choose wireless charging EV, because using plug-in charging EV under this EV charging station location plan will have a smaller travel cost.

Table 3

EV charging station location plan when budget=150 (million).

	Plug-in charging			Wireless charging	
Node No.	Level 1	Level 2	Level 3	Node	Link
2			√		10
3			√		29
5			√		
6			√		

7	√

Table 4

Objective function value and customers’ choice of EV types when budget=150 (million).

Optimal objective value	EV choice probability						
	Tour	1			2		
	User class	1	2	3	1	2	3
	Wireless Charging EV	0.53	0.51	0	0	0	0
6773.80	Plug-in charging EV	0.47	0.49	1	1	1	1

Table 5

Network equilibrium link traffic flow (veh/h) when budget=150 (million).

Link	Flow	Link	Flow	Link	Flow
1	100.0	14	0.0	27	0.0
2	0.0	15	0.0	28	50.0
3	50.0	16	100.0	29	100.0
4	0.0	17	0.0	30	50.0
5	150.0	18	0.0	31	0.0
6	0.0	19	0.0	32	0.0
7	150.0	20	100.0	33	0.0
8	0.0	21	0.0	34	0.0
9	50.0	22	50.0	35	100.0
10	100.0	23	0.0	36	0.0
11	50.0	24	150.0	37	0.0
12	0.0	25	0.0	38	0.0
13	0.0	26	150.0		

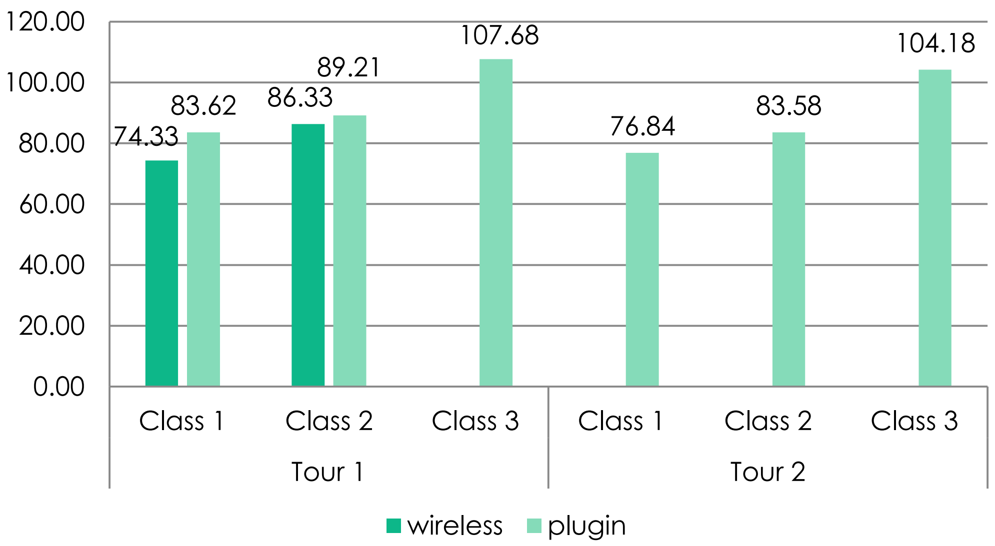

Figure 3 Minimum traveling cost of each tour and each class user.

Figure 4 illustrates the recharging plans of tour 1 Class 2 travelers using different types of EVs, who choose the same route as shown in this figure, where the numbers beside nodes or links represent the amount of electricity recharged at this node or via the wireless recharging link, the number in parenthesis represents the delay time due to recharging behavior. Note that the delay time does not include the original dwelling time at destination nodes. It can be observed that plugin charging EV tend to utilize the original dwelling time at destination nodes to recharge their batteries, for example, at node 6 and node 3. Besides, wireless charging EVs prefer dynamic recharging when they are driving on links because there is no recharging delay. What's more, only level 3charging stations are employed in this example, which indicates that plugin charging EV drivers prefer fast charging even though the charging price is higher. Finally, we notice that in this example, with a sufficiently high value of budget, wireless EVs may reduce the recharging delay to zero, i.e., they can fully utilize dynamic recharging via wireless recharging lane.

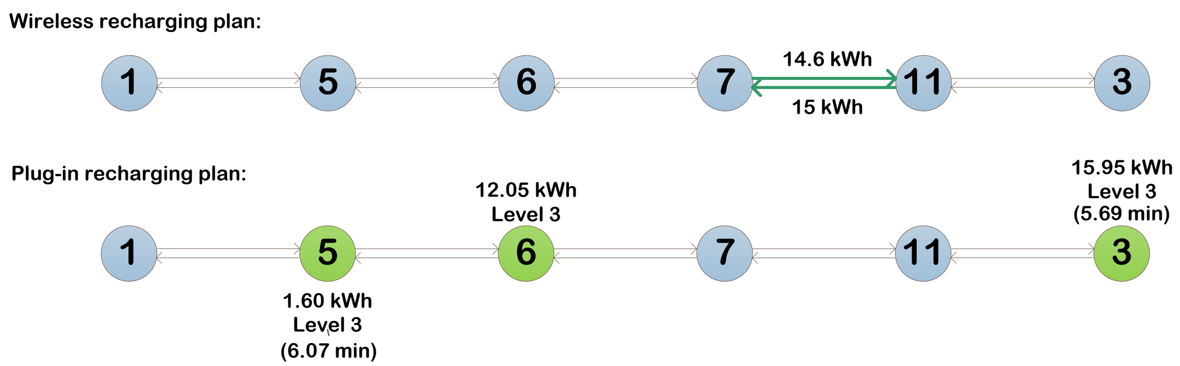

Figure 4 Recharging plans of tour 1 class 2 travlers using different EV types.

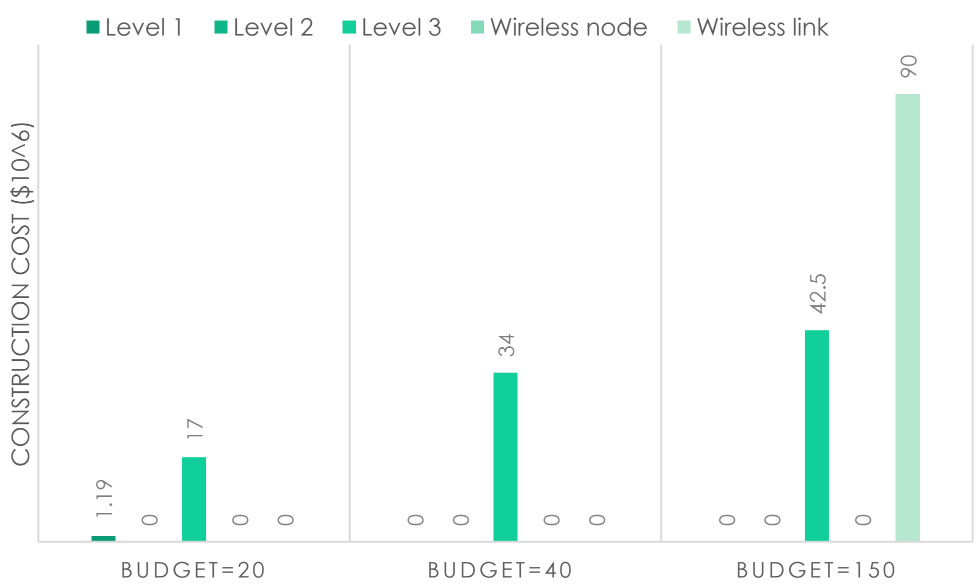

Figure 5 Comparison of construction investment assignments with different budgets.

Figure 5 compares the construction investment assignment results for three different budget cases, where the budget is set as $20 million, $40 million, and $150 million, respectively. When budget is given at a low level of 20, the solution locates a level 1 station at node 6 and level 3 stations at both node 7 and 11. No wireless charging facilities are planned and the final objective function value is 8049.22. When budget is 40, the obtained solution locates level 3 stations at node 2, 3, 6, and 7 respectively. There is no wireless charging facilities located in this case neither, thus all customers choose to use plugin charging EV. The final feasible objective function value is 6880.26. It can be observed that, similar with the result when budget is set as 150, the investment plan has its priority to construct higher level charging stations, probably because road users prefer recharging at higher level stations to avoid extra recharging delay. . What's more, in the highest budget case, the construction cost of wireless dynamic charging facilities is much more expensive, which is almost two times of the construction cost of plug-in charging stations. However, it does reduce the recharging delay time as shown in Table 6, where the average income weighted recharging cost and average recharging delay with the three given budget cases are demonstrated. Generally, higher budget can greatly reduce the plugin EV recharging delay and slightly reduce the income weighted recharging cost for class 1 users. Second, when budget is set to be 150, the income weighted recharging cost for wireless recharging EV is about 71.4%, 70.9% higher than those of plug-in charging EV for class 1 and 2 users, respectively. Meanwhile, the average recharging delay of wireless recharging EV is 0, however, plugin EV users who still have to spend extra time for recharging. Finally, it is also found that the Class 1 travelers using plugin EV have more recharging delay than Class 3 travelers, which is probably due to their higher range anxiety. In contrast, the average income weighted recharging cost of Class 1 is much lower than Class 3 users, because Class 1 users have a higher wage. It should be noted that, the result is obtained under the current setting of travelers' income, recharging prices and construction fee for multiple types of EV recharging stations. Changing of these parameters may lead to a far different result. The impact of charging price is beyond the focus of this paper and may be studied in future research.

Table 6

Average income weighted recharging cost and average recharging delay with different budgets.

		Average wage weighted recharging cost			Average recharging delay		
Budget	EV type	Class 1	Class 2	Class 3	Class 1	Class 2	Class 3
20	Plug-in EV	6.15	12.94	37.40	23.81	24.19	25.79
40	Plug-in EV	6.01	13.10	37.82	11.91	10.79	5.26
150	Plug-in EV	5.95	12.99	37.82	11.12	10.29	5.26
	Wireless EV	10.20	22.20	0	0.00	0.00	0.00

4.1.2. Performance of the presented solution algorithm

The performance of the presented solution algorithm is shown in this section. The parameters adopted in the test are show as follows. The number of binary variables in the example is 71, thus the dimensions of $\mathbf{y}$ is 71 and set $n_0 = 72$. For a better global search at beginning, the perturbing probability is initialized as $p_{slct} = 0.8$. The maximum number for counters are set as $C_{succ}^{\max} = 5$ and $C_{fail}^{\max} = 5$. $t = 30000$ candidate points are randomly generated in each iteration. The serie $(v_1, v_2, v_3) = (0.8, 0.9, 0.95)$ is adopted in determining the weight of response surface and distance.

Figure 6 shows the obtained best feasible objective function value so far from the 1st iteration to the current iteration when the presented solution algorithm is applied to the test network when budget is given at $150 million. The first feasible best objective function value is equal to a random found best feasible objective function value 8130.31 in the initialization step, which is apparently not desired. In the first iteration, a much better objective 7263.11 is immediately achieved than the one in the initialization step, which is improved by 11.9%. This is because the evaluation of $d+1$ affinely independent points in the initialization step contributes significantly to get the initial picture of the black-box objective function by the RBF interpolation. Then the best feasible objective function value slowly converges with the iteration progress. The algorithm stops after the 37$^{\text{th}}$ iteration and the final solution is obtained at the 15$^{\text{th}}$ iteration.

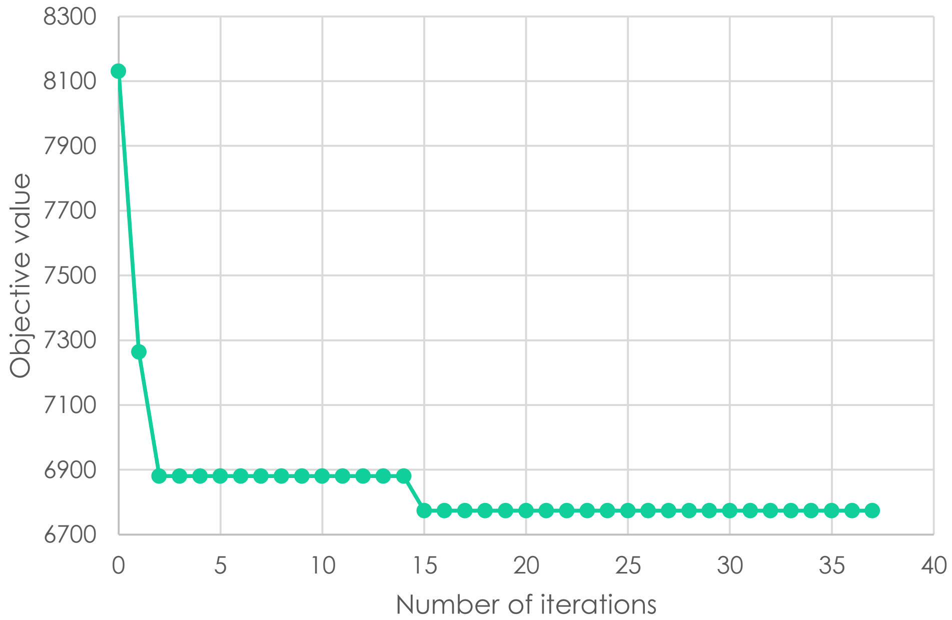

Figure 6 Objective function values of best feasible solution within 40 iterations.

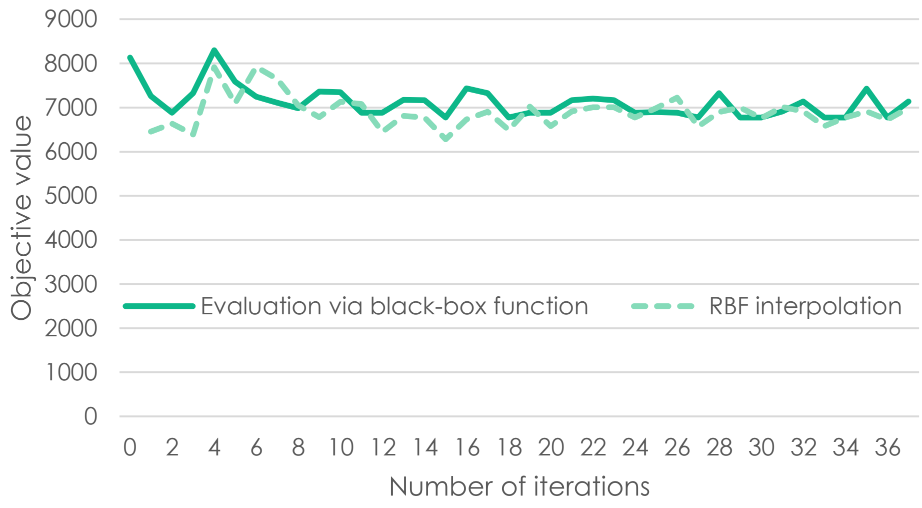

Figure 7 Comparison of objective function values between approximated value via RBF interpolation and real value via black-box function evaluation.

Figure 7 compares the approximated objective function value from the RBF interpolation with the real value from black-box objective function evaluation in each iteration. At first, the RBF model is indeed a crude approximation for the true objective. The difference between the two is quite large within the first several iterations. However, with the progress of solution procedure the approximation of RBF interpolation is improved gradually, because the new evaluation point updates the fitting in each iteration. Finally, the two lines are very close to each other in the last several iterations, which indicates that the RBF model can approximate the black-box objective function very well in the near feasible region of the current best solution.

The total calculation time for the test is about 13.47 hours, among which 93.5% is the evaluation time of the expensive black-box function. In the test example, each black-box evaluation costs about 7.53 minutes, while other procedures of the presented solution algorithm, including fitting and random points generation, costs about 0.53 minute in each iteration. It shows that the computational load for stochastic RBF-based algorithm excluding black-box function evaluation only is much lower in contrast to the evaluation of expensive black-box function.

The test network is only an illustrative example. In real world, the traffic network is much more complex, thus each evaluation of the black-box function is much more expensive than the example, which may cost hours to run the black-box function each time. In that case of situation, the presented solution algorithm should be more applicable than conventional meta-heuristic algorithms, such as genetic algorithm; basically, by using a reasonably accurate surrogate model to replace the original one, the problem is more analytically tractable and computationally cheap.

4.1.3. Comparison with result without considering EV type choice

In the tri-level programming formulation in this study, the travelers' EV type choice is explicitly considered in the middle-level program. The EV type choice, on one hand, changes after the charging facilities location plan; on the other hand, affects the resultant traffic flow pattern and thus the charging facilities siting plan. Therefore, it is essential to include it into the model formulation. To show the significance of middle-level programming, which incorporates electric vehicle demand and infrastructure interactions into the charging facilities location problem, a model without the middle-level programming is tested. The amounts of different types of electric vehicles are no longer variables but fixed constants given in priori. In this test, without loss of generality, the probabilities of choosing different types of EVs of each user class are simply set to be equal, i.e., half of each class users choose wireless recharging EV and the other half choose plug-in recharging EV. The obtained locational plan is shown in Table 7 with given budget of $150 million. The objective function value of this location plan is 7583.12, which is 11.95% higher than the result from the presented model considering EV type choice. Since both wireless and plug-in charging EVs are to be used in all tours, the location plan need siting wireless and plug-in charging facilities for both the two types of EVs. However, in this situation, the travel cost for some travelers is much higher than that of choosing another type of EV, as shown in Figure 8. For example, class 3 users of tour 2, the travel cost of using wireless EV is 54.1% higher than using plug-in charging EV. Hence, in practice, the class 3 travelers of tour 2 will probably not choose the wireless charging EV, and thus the result may be inaccurate. This test, from another aspect, justifies the necessity of considering the interactions between the EV type choice and recharging facilities location.

Table 7

EV charging station location plan when budget=150 (million) considering fixed EV choice.

	Plug-in charging			Wireless charging	
Node No.	Level 1	Level 2	Level 3	Node	Link
2			√	√	10
3			√		29
6			√	√	
7				√	

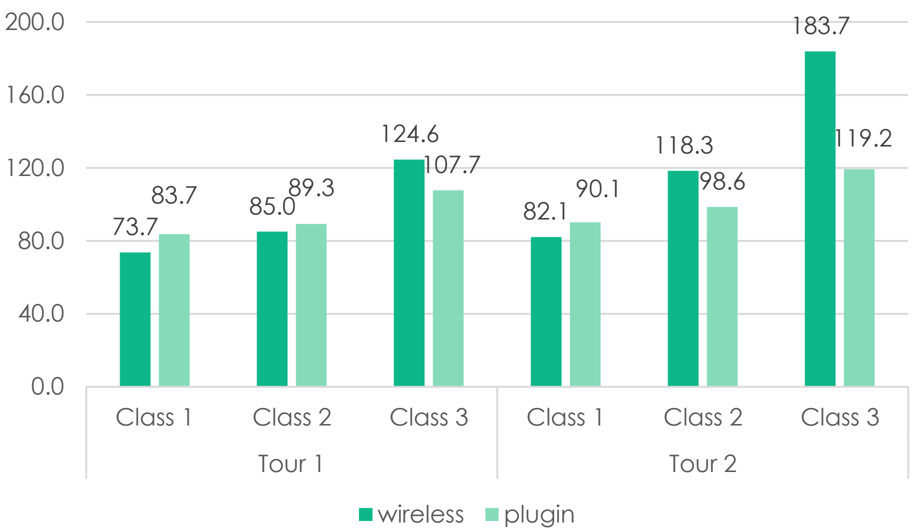

Figure 8 Minimum traveling cost of each tour and each class user with fixed EV choice.

4.2. The Sioux Falls network

The second example is tested on the well-known Sioux Falls network, which has 24 nodes and 76 links and is usually adopted as larger benchmark network in many transportation network design problems (LeBlanc, 1975; Liu and Wang, 2015; Liu et al., 2015; Suwansirikul et al., 1987). The link related input parameters of Sioux Falls network are shown in Table 8; tour information, which includes O-D pairs and dwelling time at each destination node, is listed in Table 9. The demand corresponding to each tour is set as 1000. Government budget in the test is assumed as \$80 million. Link pairs between nodes (6,8), (7,8), (9,10), (10,16) and (13,24) are available for locating dynamic charging lane on both directions. The set of nodes $\{6,11,13,15,21\}$ are available for locating both wireless charging stations and traditional plug-in charging stations of all levels. The other parameters and assumptions related to user classes, EV types and charging facilities are set identical to the parameters in the Nguyen-Dupuis test network. This test is run on a laptop with MacOS Sierra (Version 10.12.2) platform, a 2 GHz Intel Core i5 processor and 8 GB RAM. The YALMIP R20150908 with MATLAB R2014b is used to model the example and the academic version commercial solver Mosek 8 is used as an external solver of YALMIP to solve all MIPs in the test.

Table 8

Link capacity (10^3 veh/h) and free flow travel time (min).

Link	Capacity	t_a^0	Link	Capacity	t_a^0	Link	Capacity	t_a^0
1-2	4.8986	1.6	10-11	5.0501	8	17-16	4.9935	6.4
1-3	4.8986	1.6	10-15	5.0458	4	17-19	5.2299	1.6
2-1	7.8418	2.4	10-16	10.0000	4	18-7	4.8239	1.6
2-6	7.8418	2.4	10-17	5.0501	8	18-16	23.4034	1.6
3-1	13.9158	2.4	11-4	10.0000	4	18-20	19.6798	2.4

3-4	13.9158	2.4	11-10	13.5120	4.8	19-15	23.4034	3.2
3-12	5.1335	4	11-12	4.9935	6.4	19-17	15.6508	3.2
4-3	5.1335	4	11-14	4.9088	4.8	19-20	4.8239	1.6
4-5	5.0913	3.2	12-3	10.0000	4	20-18	5.0026	3.2
4-11	5.0913	3.2	12-11	4.9088	4.8	20-19	23.4034	3.2
5-4	25.9002	4.8	12-13	4.8765	3.2	20-21	5.0020	3.2
5-6	23.4034	3.2	13-12	23.4034	3.2	20-22	5.0599	4.8
5-9	25.9002	4.8	13-24	4.9088	4.8	21-20	5.0756	4
6-2	4.9581	4	14-11	25.9002	2.4	21-22	5.0599	4.8
6-5	23.4034	3.2	14-15	25.9002	2.4	21-24	5.2299	1.6
6-8	17.1105	3.2	14-23	4.8765	3.2	22-15	4.8853	2.4
7-8	23.4034	3.2	15-10	5.1275	4	22-20	10.3149	3.2
7-18	17.1105	3.2	15-14	4.9247	3.2	22-21	5.0756	4
8-6	17.7827	1.6	15-19	13.5120	4.8	22-23	5.2299	1.6
8-7	4.9088	4.8	15-22	5.1275	4	23-14	5.0000	3.2
8-9	17.7827	1.6	16-8	15.6508	3.2	23-22	4.9247	3.2
8-16	4.9479	3.2	16-10	10.3149	3.2	23-24	5.0000	3.2
9-5	10.0000	4	16-17	5.0458	4	24-13	5.0785	1.6
9-8	4.9581	4	16-18	5.2299	1.6	24-21	4.8853	2.4
9-10	4.9479	3.2	17-10	19.6798	2.4	24-23	5.0785	1.6
10-9	23.4034	1.6						

Table 9

Tour information of the Sioux Falls network.

Tour	Origin node	Destination node	Dwelling time (min)	Tour	Origin node	Destination node	Dwelling time (min)
1	1	7	72	3	4	7	60
	7	8	180		7	4	-
	8	16	70				
	16	22	113	4	8	9	60
	22	1	-		9	10	110
					10	8	-
2	8	16	120				
	16	10	15	5	20	13	36
	10	15	53		13	11	151
	15	17	120		11	3	7
	17	8	-		3	20	-

The optimal location plan of various types of EV charging facilities obtained through the developed model and presented solution algorithm is shown in Figure 9. Within the given budget, one pairs of dynamic charging lanes are located between nodes (7,8) and two static charging stations are planned for wireless charging EVs; while two level 3, two level 2 and one level 1 plug-in charging stations are located for traditional plug-in charging EVs. There will be 2103 travelers, about 42% of all travelers, choosing wireless charging EVs and the others choosing plug-in charging EVs. The optimal objective function value, i.e., total social cost, is about 9.838E+4 under this construction plan.

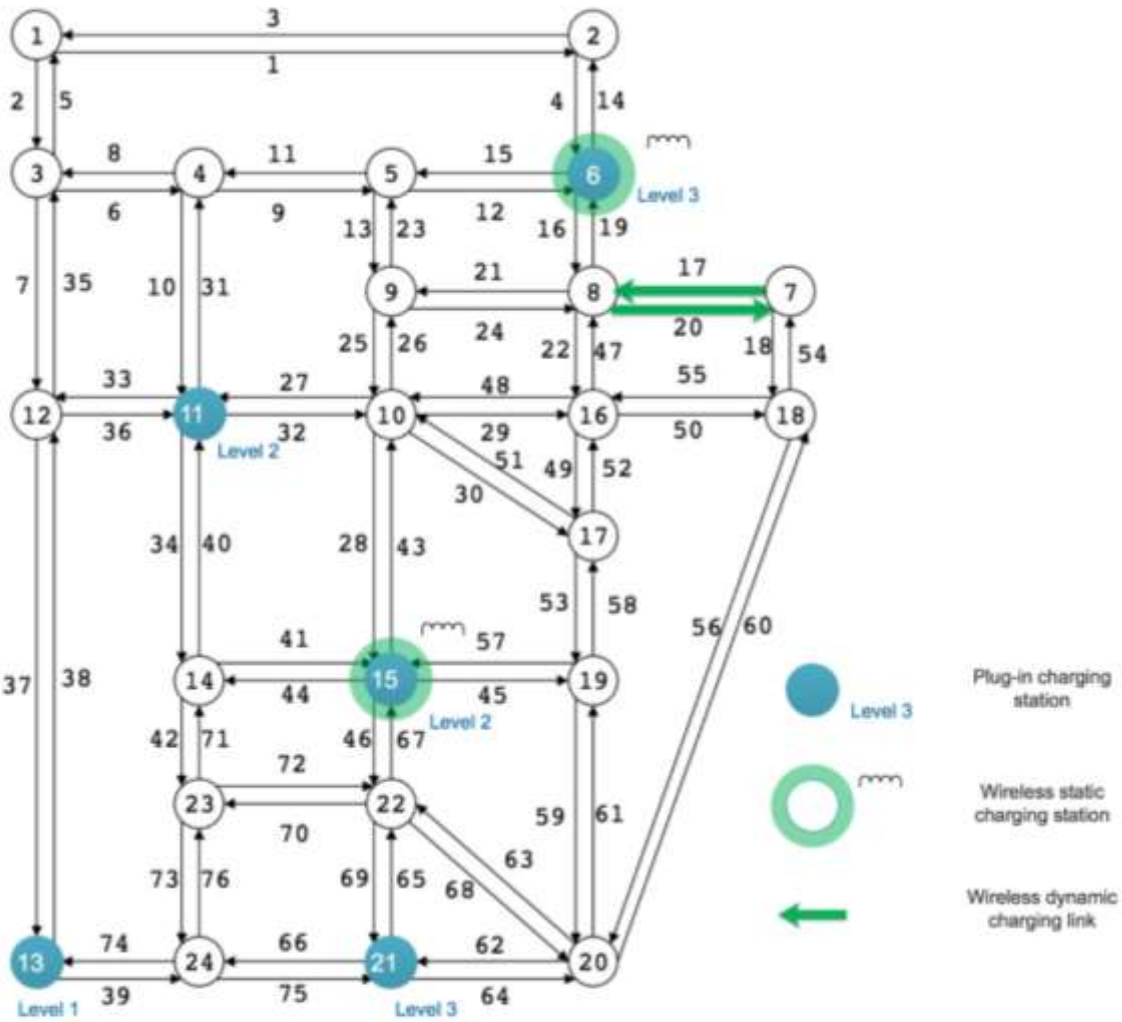

Figure 9 EV charging facilities optimal location plan of Sioux Falls network.

Figure 10 shows the percentage of wireless charging EV and plug-in charging EV users of each user class traveling on tour 1, 3 and 5. Figure 11 shows the corresponding minimum path cost of each class users. Figure 12 reports the wage weighted unit recharging fee for different user classes. Generally, the minimum path cost of class 3 users is higher than the other two class users of the same tour, because the initial state of battery and the wage rate of this class users are both lower than the other two classes and the low wage rate makes this class users more sensitive to the recharging cost, as clearly illustrated in Figure 12. Hence, it seems that the class 3 users tend to choose EV type with less path cost, though the other two class users also have the same tendency, but not as prominent as class 3 users. The difference of numbers of two EV type users for class 3 is generally bigger than that for the other two class users, as shown in Figure 10.

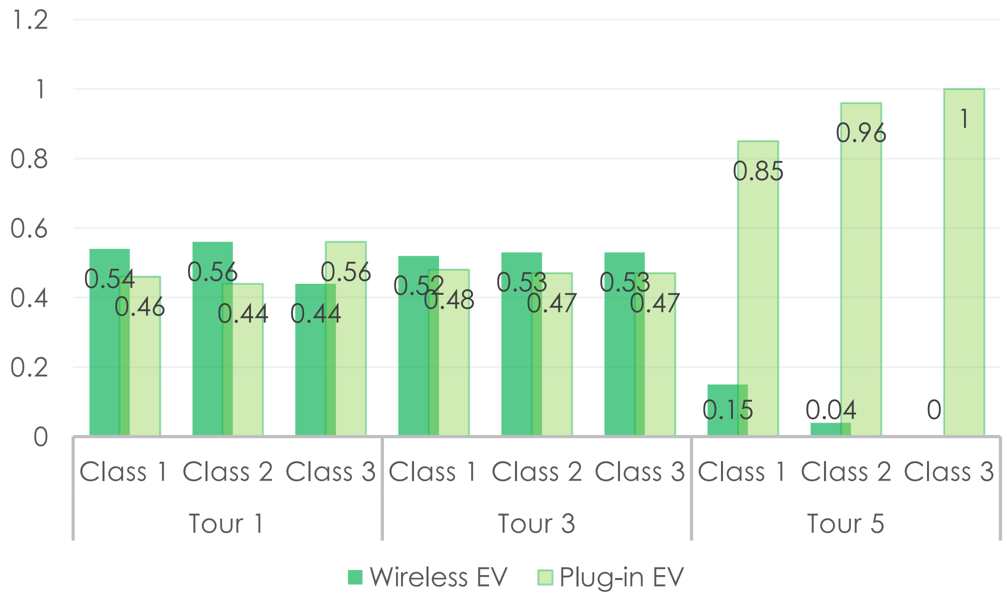

Figure 10 Percentage of users choosing different EV types of Tour 1, 3 and 5.

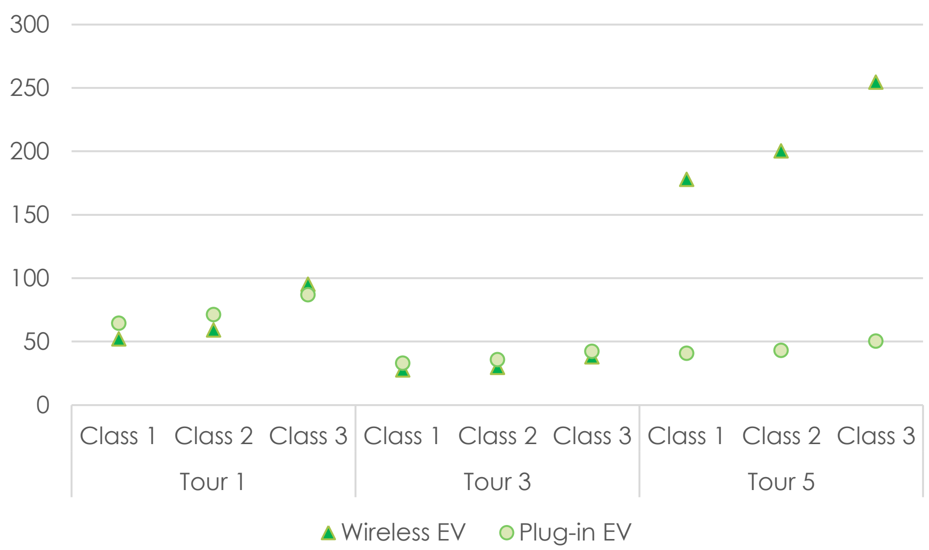

Figure 11 Minimum path cost of each class users of Tour 1, 3 and 5.

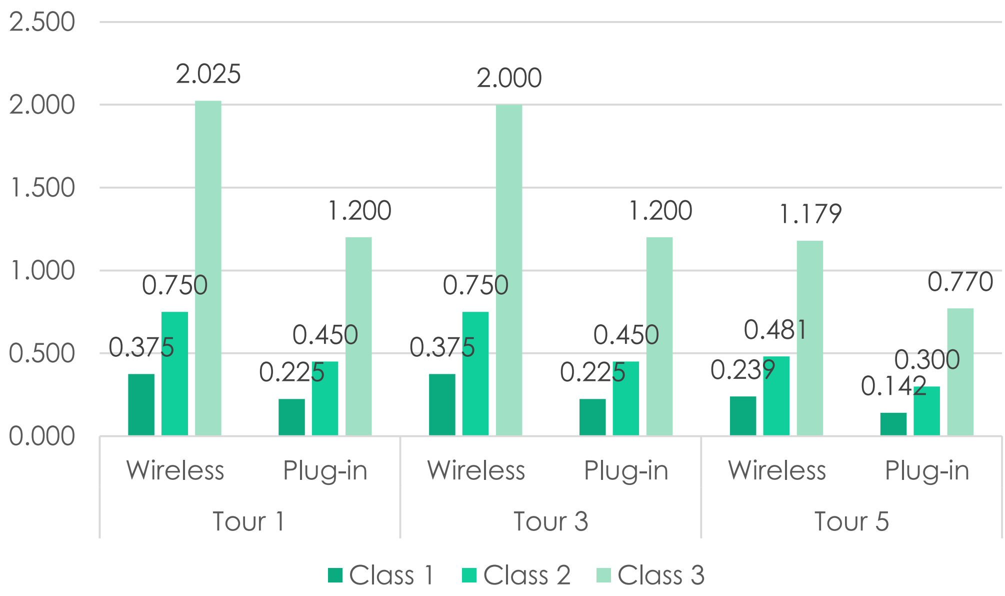

Figure 12 Wage weighted unit recharging fee for different user classes of Tour 1, 3 and 5.

Figure 13 Percentage of different classes of each EV type users.

Figure 13 reports the ratio of different classes of each EV type users to the whole system. There are about 35% of wireless EV users are class 1 users, which is the most among the three classes; on the contrary, 35% of plug-in EV users are class 3 users, which is also the most of the three classes. Figure 14 illustrates the amount of electricity recharged through different types of EV charging facilities. For wireless charging EV, about 83.9% of electricity are obtained via dynamic charging on a wireless charging lane; as for plug-in charging EV, 54.8% of electricity are recharged through level 2 charging stations and 42.7% through level

3 charging stations. Hence, it seems that consumers would like to choose higher level charging stations from the result of this test. The calculation time of this test is about 8 hours.

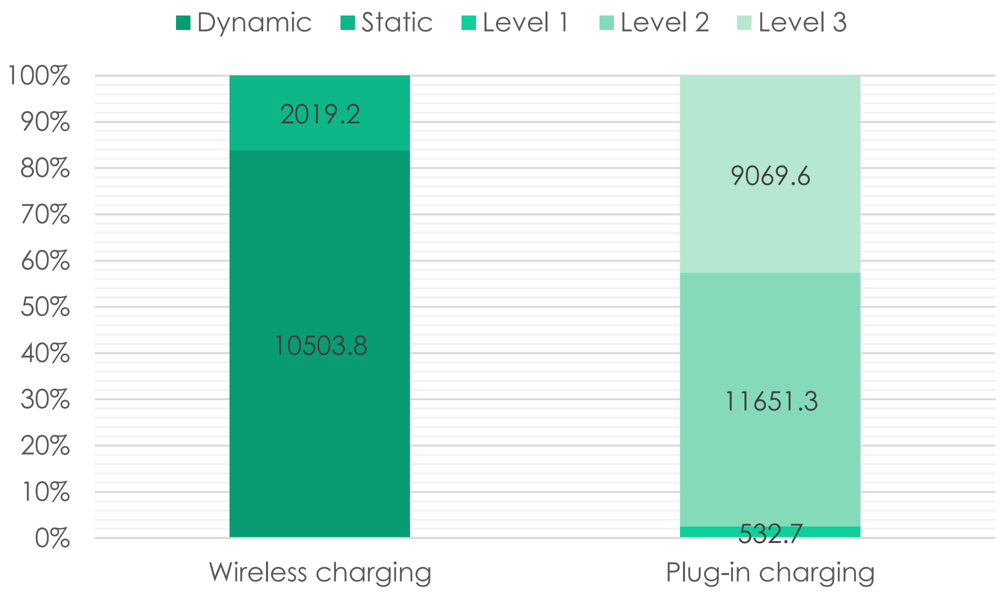

Figure 14 Amount of electricity (kWh) recharged through different types of EV charging facilities.

5. Conclusions

In this paper, we propose a modeling framework for locating multiple types of BEV charging facilities that aims to assist the government planners to make better decisions. The presented model considers the recently fast developing wireless static and dynamic charging in the decision procedure. Besides, two types of road users' behavior, i.e., vehicle choice between different types of BEVs and different classes of BEV users' routing choice, are considered in the model framework. The presented complicated tri-level model is then treated as black-box optimization and solved by an efficient stochastic radial basis function response surface model based algorithm. The inherent time-consuming black-box function is solved by applying a combined fixed-point method and an MSA method. Two shortest-path-finding sub-problems for wireless charging EV and plug-in charging EV, respectively, are developed and embedded in the MSA solution procedure. Numerical tests show that the location plan can be obtained from the developed model and the presented solution algorithm.

Acknowledgements

This study is sponsored by the Singapore Ministry of Education Academic Research Fund Tier 1 Grant RG117/14 (M401030000).

References:

Adler, J.D., Mirchandani, P.B., 2014. Online routing and battery reservations for electric vehicles with swappable batteries. Transportation Research Part B 70, 285-302.
Boukouvala, F., Hasan, M.M.F., Floudas, C.A., 2015. Global optimization of general constrained grey-box models: New method and its application to constrained pdes for pressure swing adsorption. Journal of Global Optimization, 1-40.
Budhia, M., Boys, J.T., Covic, G.A., Huang, C.Y., 2013. Development of a single-sided flux magnetic coupler for electric vehicle ipt charging systems. IEEE Transactions on Industrial Electronics 60 (1), 318-328.
Capar, I., Kuby, M., Leon, V.J., Tsai, Y.-J., 2013. An arc cover–path-cover formulation and strategic analysis of alternative-fuel station locations. European Journal of Operational Research 227 (1), 142-151.
Chawla, N., Tosunoglu, S., 2012. State of the art in inductive charging for electronic appliances and its future in transportation, 2012 Florida Conference on Recent Advances in Robotics, Boca Raton, Florida, pp. 1-7.
Chen, F., Taylor, N., Kringos, N., 2015a. Electrification of roads: Opportunities and challenges. Applied Energy 150, 109-119.
Chen, L., Nagendra, G.R., Boys, J.T., Covic, G.A., 2015b. Double-coupled systems for ipt roadway applications. IEEE Journal of Emerging and Selected Topics in Power Electronics 3 (1), 37-49.
Chen, X.M., Zhang, L., He, X., Xiong, C., Li, Z., 2014. Surrogate- based optimization of expensive- to- evaluate objective for optimal highway toll charges in transportation network. Computer- Aided Civil and Infrastructure Engineering 29 (5), 359-381.
Chen, Z., He, F., Yin, Y., 2016. Optimal deployment of charging lanes for electric vehicles in transportation networks. Transportation Research Part B 91, 344-365.
Church, R., ReVelle, C., 1974. The maximal covering location problem. Papers of the Regional Science Association 32 (1), 101-118.
Cressie, N., 2015. Statistics for spatial data. John Wiley & Sons.
Dafermos, S.C., 1971. An extended traffic assignment model with applications to two-way traffic. Transportation Science 5 (4), 366-389.
Dafermos, S.C., 1972. The traffic assignment problem for multiclass-user transportation networks. Transportation science 6 (1), 73-87.
Daskin, M.S., 2008. What you should know about location modeling. Naval Research Logistics (NRL) 55 (4), 283-294.
Deloitte, 2011. Unplugged: Electric vehicle realities versus consumer expectations.
Du, B., Wang, D.Z.W., 2014. Continuum modeling of park-and-ride services considering travel time reliability and heterogeneous commuters – a linear complementarity system approach. Transportation Research Part E 71, 58-81.
Farahani, R.Z., Asgari, N., Heidari, N., Hosseininia, M., Goh, M., 2012. Covering problems in facility location: A review. Computers & Industrial Engineering 62 (1), 368-407.
Farahani, R.Z., Miandoabchi, E., Szeto, W.Y., Rashidi, H., 2013. A review of urban transportation network design problems. European Journal of Operational Research 229 (2), 281-302.
Fowler, K.R., Reese, J.P., Kees, C.E., Dennis, J.E., Kelley, C.T., Miller, C.T., Audet, C., Booker, A.J., Couture, G., Darwin, R.W., 2008. Comparison of derivative-free optimization methods for groundwater supply and hydraulic capture community problems. Advances in Water Resources 31 (5), 743-757.
Fuller, M., 2016. Wireless charging in california: Range, recharge, and vehicle electrification. Transportation Research Part C 67, 343-356.
Gurobi Optimization, 2016. Gurobi optimizer reference manual, http://www.gurobi.com.
Haghbin, S., Khan, K., Lundmark, S., Alaküla, M., Carlson, O., Leksell, M., Wallmark, O., 2010. Integrated chargers for ev's and phev's: Examples and new solutions, Electrical Machines (ICEM), 2010 XIX International Conference on. IEEE, pp. 1-6.
Hale, T.S., Moberg, C.R., 2003. Location science research: A review. Ann Oper Res 123 (1), 21-35.
He, F., Wu, D., Yin, Y., Guan, Y., 2013a. Optimal deployment of public charging stations for plug-in hybrid electric vehicles. Transportation Research Part B 47, 87-101.
He, F., Yin, Y., Lawphongpanich, S., 2014. Network equilibrium models with battery electric vehicles. Transportation Research Part B 67, 306-319.

He, F., Yin, Y., Zhou, J., 2013b. Integrated pricing of roads and electricity enabled by wireless power transfer. Transportation Research Part C 34, 1-15.

He, F., Yin, Y., Zhou, J., 2015. Deploying public charging stations for electric vehicles on urban road networks. Transportation Research Part C 60, 227-240.

Hodgson, M.J., 1990. A flow-capturing location-allocation model. Geographical Analysis 22 (3), 270-279.

Huang, Y., Li, S., Qian, Z.S., 2015. Optimal deployment of alternative fueling stations on transportation networks considering deviation paths. Networks and Spatial Economics 15 (1), 183-204.

Jang, Y.J., Jeong, S., Ko, Y.D., 2015. System optimization of the on-line electric vehicle operating in a closed environment. Computers & Industrial Engineering 80, 222-235.

Jang, Y.J., Ko, Y.D., Jeong, S., 2012. Optimal design of the wireless charging electric vehicle, Electric Vehicle Conference (IEVC), 2012 IEEE International, pp. 1-5.

Jang, Y.J., Suh, E.S., Kim, J.W., 2016. System architecture and mathematical models of electric transit bus system utilizing wireless power transfer technology. IEEE Systems Journal 10 (2), 495-506.

Jiang, N., Xie, C., 2013. Computing and analyzing equilibrium network flows of gasoline and electric vehicles, Transportation Research Board 92nd Annual Meeting.

Jiang, N., Xie, C., Duthie, J.C., Waller, S.T., 2014. A network equilibrium analysis on destination, route and parking choices with mixed gasoline and electric vehicular flows. EURO Journal on Transportation and Logistics 3 (1), 55-92.

Jiang, N., Xie, C., Waller, S., 2012. Path-constrained traffic assignment. Transportation Research Record: Journal of the Transportation Research Board 2283, 25-33.

Jiang, Y., Szeto, W.Y., Long, J., Han, K., 2016. Multi-class dynamic traffic assignment with physical queues: Intersection-movement-based formulation and paradox. Transportmetrica A: Transport Science 12 (10), 878-908.

Kim, J.-G., Kuby, M., 2012. The deviation-flow refueling location model for optimizing a network of refueling stations. International Journal of Hydrogen Energy 37 (6), 5406-5420.

Kim, J.-G., Kuby, M., 2013. A network transformation heuristic approach for the deviation flow refueling location model. Comput. Oper. Res. 40 (4), 1122-1131.

Ko, Y.D., Jang, Y.J., 2013. The optimal system design of the online electric vehicle utilizing wireless power transmission technology. IEEE Transactions on Intelligent Transportation Systems 14 (3), 1255-1265.

Ko, Y.D., Jang, Y.J., Jeong, S., 2012. Mathematical modeling and optimization of the automated wireless charging electric transportation system, 2012 IEEE International Conference on Automation Science and Engineering (CASE), pp. 250-255.

Ko, Y.D., Jang, Y.J., Lee, M.S., 2015. The optimal economic design of the wireless powered intelligent transportation system using genetic algorithm considering nonlinear cost function. Computers & Industrial Engineering 89, 67-79.

Kuby, M., Lim, S., 2005. The flow-refueling location problem for alternative-fuel vehicles. Socio-Economic Planning Sciences 39 (2), 125-145.

Kuby, M., Lim, S., 2007. Location of alternative-fuel stations using the flow-refueling location model and dispersion of candidate sites on arcs. Networks and Spatial Economics 7 (2), 129-152.

LeBlanc, L.J., 1975. An algorithm for the discrete network design problem. Transportation Science 9 (3), 183-199.

Lee, Y.-G., Kim, H.-S., Kho, S.-Y., Lee, C., 2014. User equilibrium-based location model of rapid charging stations for electric vehicles with batteries that have different states of charge. Transportation Research Record: Journal of the Transportation Research Board 2454, 97-106.

Lim, S., Kuby, M., 2010. Heuristic algorithms for siting alternative-fuel stations using the flow-refueling location model. European Journal of Operational Research 204 (1), 51-61.

Liu, H., Wang, D.Z.W., 2015. Global optimization method for network design problem with stochastic user equilibrium. Transportation Research Part B 72, 20-39.

Liu, H., Wang, D.Z.W., Yue, H., 2015. Global optimization for transport network expansion and signal setting. Mathematical Problems in Engineering 2015.

Löfberg, J., 2004. Yalmip : A toolbox for modeling and optimization in matlab, Proceedings of the 2004 IEEE International Symposium on Computer Aided Control Systems Design, Taipei, Taiwan, pp. 284-289.

Nguyen, S., Dupuis, C., 1984. An efficient method for computing traffic equilibria in networks with asymmetric transportation costs. Transportation Science 18 (2), 185-202.
Nie, Y., Ghamami, M., Zockaie, A., Xiao, F., 2016. Optimization of incentive polices for plug-in electric vehicles. Transportation Research Part B 84, 103-123.
Onar, O.C., Miller, J.M., Campbell, S.L., Coomer, C., White, C.P., Seiber, L.E., 2013. Oak ridge national laboratory wireless power transfer development for sustainable campus initiative, Transportation Electrification Conference and Expo (ITEC), 2013 IEEE, pp. 1-8.
Pelletier, S., Jabali, O., Laporte, G., 2014. Battery electric vehicles for goods distribution: A survey of vehicle technology, market penetration, incentives and practices.
Powell, M.J., 1992. The theory of radial basis function approximation in 1990, Advances in numerical analysis: Wavelets, subdivision, and radial functions. Oxford University Press, Oxford, pp. 105-210.
Regis, R.G., 2011. Stochastic radial basis function algorithms for large-scale optimization involving expensive black-box objective and constraint functions. Comput. Oper. Res. 38 (5), 837-853.
Regis, R.G., Shoemaker, C.A., 2007. A stochastic radial basis function method for the global optimization of expensive functions. INFORMS Journal on Computing 19 (4), 497-509.
Riemann, R., Wang, D.Z.W., Busch, F., 2015. Optimal location of wireless charging facilities for electric vehicles: Flow-capturing location model with stochastic user equilibrium. Transportation Research Part C 58, Part A, 1-12.
Sherali, H.D., Adams, W.P., 1999. A reformulation-linearization technique for solving discrete and continuous nonconvex problems. Kluwer Academic Publishers, Dordrecht, Netherlands.
Suwansirikul, C., Friesz, T.L., Tobin, R.L., 1987. Equilibrium decomposed optimiztion: A heuristic for the continuous equilibrium network design problem. Transportation Science 21 (4), 254-263.
Upchurch, C., Kuby, M., Lim, S., 2009. A model for location of capacitated alternative-fuel stations. Geographical Analysis 41 (1), 85-106.
Wan, X., Pekny, J.F., Reklaitis, G.V., 2005. Simulation-based optimization with surrogate models—application to supply chain management. Computers & chemical engineering 29 (6), 1317-1328.
Wang, D., Du, B., 2013. Reliability-based modeling of park-and-ride service on linear travel corridor. Transportation Research Record: Journal of the Transportation Research Board 2333, 16-26.
Wang, D.Z.W., Du, B., 2016. Continuum modelling of spatial and dynamic equilibrium in a travel corridor with heterogeneous commuters—a partial differential complementarity system approach. Transportation Research Part B 85, 1-18.
Wang, Y.-W., Lin, C.-C., 2009. Locating road-vehicle refueling stations. Transportation Research Part E 45 (5), 821-829.
Wardrop, J.G., 1952. Some theoretical aspects of road traffic research, Proceedings of the Institution of Civil Engineers, pp. Part II, Vol. 1, 325-378.
Wu, H.H., Gilchrist, A., Sealy, K., Israelsen, P., Muhs, J., 2011. A review on inductive charging for electric vehicles, 2011 IEEE International Electric Machines & Drives Conference (IEMDC), pp. 143-147.
Yilmaz, M., Krein, P.T., 2013. Review of battery charger topologies, charging power levels, and infrastructure for plug-in electric and hybrid vehicles. IEEE Transactions on Power Electronics 28 (5), 2151-2169.